Sex-peptide targets distinct higher order processing neurons in the brain to induce the female post-mating response

MOHANAKARTHIK P. NALLASIVAN[1], DEEPANSHU N.D. SINGH[2], MOHAMMED SYAHIR R. S. SALEH[1] AND MATTHIAS SOLLER[1,2,3]

[1]School of Biosciences, College of Life and Environmental Sciences, University of Birmingham, Edgbaston, Birmingham, B15 2TT, United Kingdom

[2]Division of Molecular and Cellular Function, School of Biological Sciences, University of Manchester, Oxford Road, Manchester M13 9PT, United Kingdom

Running title: SP targets CNS neurons

Key Words: sex peptide, post-mating behaviors, neuronal wiring, sex peptide receptor (SPR), *fruitless* (*fru*), *doublesex* (*dsx*) and *pickpocket* (*ppk*) neurons

[3]Corresponding author: mathias.soller@manchester.ac.uk

Abstract

Sex-peptide (SP) transferred during mating induces female post-mating responses including refractoriness to re-mate and increased oviposition in *Drosophila*. Yet, where SP-target neurons reside, remained uncertain. Here we show that expression of membrane-tethered SP (mSP) pre-dominantly in the head or trunk either reduces receptivity or increases oviposition, respectively. Using fragments from large regulatory regions of *Sex Peptide Receptor*, *fruitless* and *doublesex* genes together with intersectional expression of mSP, we identified distinct interneurons in the brain and abdominal ganglion controlling receptivity and oviposition. These SP Response Inducing Neurons (SPRINz) can induce post-mating responses through SP received by mating. Trans-synaptic mapping of neuronal connections reveals input from sensory processing neurons and two post-synaptic trajectories as output. Hence, SP-target neurons operate as key integrators of sensory information for decision of behavioural outputs. Multi-modularity of SP-targets further allows females to adjust SP-mediated male manipulation to physiological state and environmental conditions for maximizing reproductive success.

Introduction

Reproductive behaviors are to a large degree hard-wired in the brain to guarantee reproductive success making the underlying neuronal circuits amenable to genetic analysis (Dulac and Kimchi 2007; Yamamoto and Koganezawa 2013; Anderson 2016; Rings and Goodwin 2019).

During development, sex-specific circuits are built into the brain under the control of the sex determination genes *doublesex* (*dsx*) and *fruitless* (*fru*) in *Drosophila* (Schutt and Nothiger 2000; Billeter et al. 2006). They encode transcription factors that are alternatively spliced in a male or female specific mode (Schutt and Nothiger 2000). By default, the *dsx* gene generates the male-specific isoform Dsx^{M}, while a female-specific isoform Dsx^{F} is generated by alternative splicing and expressed in about ~700 distinct neurons in the brain important for female reproductive behaviors directing readiness to mate and egg laying (Rideout et al. 2010; Rezaval et al. 2012). Fru^{M} is expressed in about ~1000 neurons in males and implements development of neuronal circuitry key to display male courtship behavior, but is switched off in females through alternative splicing by incorporation of a premature stop codon (Demir and Dickson 2005; Manoli et al. 2005; Stockinger et al. 2005).

The circuitry of female specific behaviors including receptivity to courting males for mating and egg laying have been mapped using intersectional gene expression via the *split-GAL4* system to restrict expression of activators or inhibitors of neuronal activity to very few neurons (Aranha and Vasconcelos 2018; Wang et al. 2020a; Wang et al. 2020b; Wang et al. 2021; Cury and Axel 2023). Through this approach, sensory neurons in the genital tract have been identified as key signal transducers for the readiness to mate and the inhibition of egg laying connecting to central parts of the brain via projection to abdominal ganglion neurons (Hasemeyer et al. 2009; Yang et al. 2009; Rezaval et al. 2012; Feng et al. 2014). This circuit

then projects onto centrally localized pattern generators in the brain to direct a behavioral response via efferent neurons (Wang et al. 2020a; Wang et al. 2020b; Wang et al. 2021).

Once females have mated, they will reject courting males and lay eggs (Manning 1967). Post-mating responses (PMRs) are induced by male derived sex-peptide (SP) and other substances transferred during mating (Chen et al. 1988; Avila et al. 2011; Hopkins and Perry 2022; Kim et al. 2024; Singh and Soller 2025). In addition to refractoriness to remate and oviposition, SP will induce a number of other behavioral and physiological changes including increased egg production, feeding, a change in food choice, sleep, memory, constipation, midgut morphology, stimulation of the immune system, and sperm storage and release (Soller et al. 1999; Peng et al. 2005; Carvalho et al. 2006; Domanitskaya et al. 2007; Kim et al. 2010; Ribeiro and Dickson 2010; Scheunemann et al. 2019) (Cognigni et al. 2011) (Avila et al. 2010; Isaac et al. 2010; Wainwright et al. 2021; White et al. 2021). SP binds to broadly expressed Sex Peptide Receptor (SPR), an ancestral receptor for myoinhibitory peptides (MIPs) (Yapici et al. 2008; Kim et al. 2010; Jang et al. 2017). Although MIPs seem not to induce PMRs, excitatory activity of MIP expressing neurons underlies re-mating (Yapici et al. 2008; Kim et al. 2010; Jang et al. 2017). Expression of membrane-tethered SP (mSP) induces PMRs in an autocrine fashion when expressed in neurons, but not glia (Nakayama et al. 1997; Haussmann et al. 2013).

First attempts to identify SP target neurons by enhancer *GAL4* induced expression of *UASmSP* only identified lines with broad expression in the nervous system (Nakayama et al. 1997). Later, drivers with more restricted expression including *dsx*, *fru* and *pickpocket* (*ppk*) genes were identified, but they are expressed in all parts of the nervous system throughout the body eluding to reveal the location of SP target sites unambiguously (Yapici et al. 2008; Hasemeyer et al. 2009; Yang et al. 2009; Rezaval et al. 2012; Haussmann et al. 2013).

To delineate where in the *Drosophila* SP target neurons are located which induce the main PMRs, refusal to mate and egg laying, we expressed mSP pre-dominantly in the head or trunk. These experiments separate reduction of receptivity induced in the head from trunk induction of egg laying. To further restrict our search for SP target neurons, we focused on three genes, *SPR*, *dsx* and *fru*, because SPR is broadly expressed but anticipated to induce PMRs only from few neurons, and because *GAL4* inserted in the endogenous *dsx* and *fru* loci induces PMRs from mSP expression. Using *GAL4* tiling lines with fragments encompassing the regulatory regions of complex *SPR*, *fru* and *dsx* genes (Pfeiffer et al. 2008; Jenett et al. 2012; Kvon et al. 2014), we identified one regulatory region in each gene reducing receptivity and inducing egg laying upon mSP expression, and one additional region in *SPR* only inducing egg laying. To further refine this analysis, we used intersectional gene expression using *split-GAL4* and *flipase* (*flp*) mediated excision of stop cassettes in *UAS* reporters (Struhl and Basler 1993; Luan et al. 2006). Consistent with previous results that the SP response can be induced via multiple pathways (Haussmann et al. 2013), we found distinct sets of SP Response Inducing Neurons (SPRINz) in the central brain and the abdominal ganglion that can induce PMRs via expression of mSP either reducing receptivity and inducing egg laying, or affecting only one of these PMRs. In contrast, we identified genital tract neuron expressing lines including *splitGAL4 nSyb* ∩ *ppk* that did not induce PMRs by expression of mSP. Likewise, we find expression of mSP or neuronal activation in head Sex Peptide Sensing Neurons (SPSN) neurons can induce PMRs. Mapping the pre- and post-synaptic connections of the distinct SP target neurons by *retro*- and *trans*-Tango (Talay et al. 2017; Sorkaç et al. 2023) revealed that SP target neurons direct higher order sensory processing in the central brain. These neurons feed into two common post-synaptic neuronal subtypes indicating that SP interferes with the integration of diverse sensory inputs to build a stereotyped output either reducing receptivity and/or increasing egg laying.

Results

Reduction of receptivity and induction of egg laying are separable by head and trunk expression of membrane-tethered SP

Due to the complex behavioral and physiological changes induced by SP, neurons in the central nervous system have been suspected as main targets for SP (Kubli 1992). To express mSP only in the head we used an *elav FRTstopFRT GAL4* in combination with *otdflp*, that expresses in the head to drive recombination and head-specific expression of mSP from *UAS* (Figure 1A, Figures S1A-F) (Haussmann et al. 2008; Asahina et al. 2014; Zaharieva et al. 2015; Nallasivan et al. 2021). To express mSP predominantly in the trunk we used *tshGAL4* (Figure 1B, Figures S1G-L) (Soller et al. 2006).

When we expressed mSP in the head, females reduced receptivity indistinguishable from mated females, but did not lay eggs, thereby again demonstrating that the two main PMRs can be separated (Figures 1C and 1D) (Haussmann et al. 2013). In contrast, when we expressed mSP in the trunk, females remained receptive, but laid eggs in numbers indistinguishable from mated females (Figures 1C and 1D).

Moreover, *tshGAL4* is expressed in *fru*, *dsx*, *ppk* genital tract sensory neurons (Figures 1E-1H). Since mSP expression with *tshGAL4* does not affect receptivity, these genital tract neurons unlikely are direct targets for SP (Haussmann et al. 2013). Taken together, these results indicate presence of SP target neurons in the brain and ventral nerve cord (VNC) for the reduction of receptivity and induction of egg laying, respectively.

Few restricted regulatory regions in large *SPR*, *fru* and *dsx* genes can induce the SP response

Expression of mSP from *UAS* via *GAL4* inserts in *fru* and *dsx* genes induces a robust reduction in receptivity and increase in egg laying (Rezaval et al. 2012; Haussmann et al. 2013). To identify SP target neurons, we thought to dissect the broad expression pattern of complex *SPR*, *fru* and *dsx* genes spanning 50-80 kb by identifying regulatory DNA fragments in the enhancer regions that drive *UAS mSP* in a subset of neurons. For these experiments, we analysed 22, 27 and 25 *GAL4* lines from the VDRC and Janelia tiling *GAL4* projects (Pfeiffer et al. 2008; Jenett et al. 2012; Kvon et al. 2014) (Figures 2A-2C).

Strikingly, in *SPR*, *fru* and *dsx* genes we identified only one regulatory region in each gene (*SPR8*, *fru11/12* and *dsx24*) that reduced receptivity and induced egg laying through *GAL4 UAS* expression of mSP (Figures 2D and 2E). In addition, we identified one line (*SPR12*) in the *SPR* gene, that induced egg laying, but did not reduce receptivity consistent with previous results that SP regulation of receptivity and egg laying can be split (Haussmann et al. 2013).

All of these lines expressed in subsets of neurons in the central brain and the ventral nerve cord in distinct, but reduced patterns compared to the expression of the *SPR*, *fru* and *dsx* genes (Yapici et al. 2008; Rideout et al. 2010; Zhou et al. 2014) (Figures 2F-2O). Moreover, these lines showed prominent labelling of abdominal ganglion neurons in the VNC (Figures 2K-2O). In addition, all of these lines except *SPR12* are also expressed in genital tract sensory neurons (Figure S2).

From all the 74 lines that we have analyzed for PMRs from *SPR*, *fru* and *dsx* genes, we also analysed expression in genital tract sensory neurons as they had been postulated to be the primary targets of SP (Yapici et al. 2008; Hasemeyer et al. 2009; Yang et al. 2009; Rezaval et al. 2012). Apart from PMR inducing lines *SPR8*, *fru11*, *fru12* and *dsx24*, that showed expression in genital tract sensory neurons, we identified three lines (*SPR3*, *SPR 21*

and *fru9*), which also robustly expressed in genital tract sensory neurons but did not induce PMRs from expression of mSP (Figure S3, S4E, S4F, S4I and S4J).

Secondary ascending abdominal ganglion neurons can induce the PMRs from mSP expression

A screen aiming to identify neurons involved in the control of receptivity and egg laying by expression of the rectifying potassium channel Kir2.1 identified six enhancer *GAL4* driver lines (*FD1-6*) (Feng et al. 2014). *FD1-6* are expressed in diverse subsets of neurons in the brain and the ventral nerve cord, in particular they show common expression in the abdominal ganglion with projections to the central brain. The lines expressing in FD1-5 neurons have been termed SAG (secondary ascending abdominal ganglion neurons) neurons, that are also interconnected with myoinhibitory peptide sensing neurons (Jang et al. 2017). Since enhancer lines identified in *SPR*, *fru* and *dsx* genes are prominently expressed in the abdominal ganglion, we tested whether mSP expression from these FD1-6 lines induced PMRs.

From these six lines, one robustly suppressed receptivity and induced egg laying (*FD6/VT003280*), while two lines only induced egg laying (*FD3/VT4515* and *FD4/V000454*) similar to controls from mSP expression (Figure 3). Again, all three lines also expressed in subsets of neurons in the central brain and VNC, particularly in the abdominal ganglion (Zhou et al. 2014). In addition, *FD3* and *FD4* did not express in genital tract sensory neurons, in contrast to *FD6* (Feng et al. 2014). A *SAG1 split-GAL4* (*VT050405/FD1 AD* and *VT007068/FD2 DBD*) did not show a response to expression of mSP and virgin females, e.g. they mated and did not lay eggs (Figure 3).

Intersectional expression reveals distinct mSP responsive neurons in the central brain and abdominal ganglion

To further restrict the expression to fewer neurons, we intersected the expression patterns of those lines that induced robust reduction of receptivity and increase of egg laying using *split-GAL4* (*SPR8*, *fru11/12*, *dsx* and *FD6*, for further experiments we used *dsxGAL4-DBD*, because *dsx24* is less robust and *fru11* and *fru12* were made into one fragment) that activates the *UAS* reporter when *GAL4* is reconstituted via dimerization of activation (AD-GAL4) and DNA binding (GAL4-DBD) domains (Luan et al. 2006) (Figure 4A).

Again, intersection of *SPR8* with *fru11/12*, *dsx* or *FD6*, and *fru11/12* with *dsx* or *FD6* expression robustly reduced receptivity and increased egg laying upon expression of mSP (Figures 4B and 4C). Accordingly, we termed these neurons SP Response Inducing Neurons (SPRINz), though the exact identity in the *splitGAL4* intersection population needs to be determined.

When we further analyzed the expression of these *split-GAL4* intersections in the brain, we found that each combination first showed very restricted expression, but second, that none of these combinations labeled the same neurons (Figures 4D-4H). For *dsx* neurons, *split-GAL4* intersections correspond to a subset of dPC2l (*SPR8* ∩ *dsx*) and dPCd-2 (*fru11/12* ∩ *dsx*) neurons (Deutsch et al. 2020; Schretter et al. 2020; Nojima et al. 2021). These results suggest the SP targets interneurons in the brain that feed into higher processing centers from different entry points likely representing different sensory input.

In the ventral nerve cord, we found expression in the abdominal ganglion with all *split-GAL4* combinations (Figures 4I-4M). In particular, intersection of *dsx* with *SPR8* or *fru11/12* showed exclusive expression in the abdominal ganglion, while the other combinations also expressed in other cells of the VNC. All together, these data suggest that

the abdominal ganglion harbors several distinct type of neurons involved in directing PMRs (Oliveira-Ferreira et al. 2023).

In the female genital tract, these *split-Gal4* combinations show expression in genital tract neurons with innervations running along oviduct and uterine walls (Figures S5A-S5E). In addition, *SPR8 ∩ fru11/12* and *SPR8 ∩ dsx* were also expressed in the spermathecae (Figures S5A-S5B).

mSP responsive neurons rely on SPR and are required for PMRs induced by SP delivered through mating

Next, we tested whether PMRs induced by mSP expression in the *SPR8 ∩ dsx*, *fru11/12 ∩ dsx* or *SPR8 ∩ fru11/12* rely on *SPR*. Expression of mSP in *dsx ∩ SPR8* and *dsx ∩ fru11/12* neurons in *SPR* mutant females did not reduce receptivity or induce egg laying (Figures 5A and B, see also Figures 4A and B), while a partial response was observed for *SPR8 ∩ fru 11/12* induced mSP expression in *SPR* mutant females, which is consistent with presence of additional receptors for SP (Haussmann et al. 2013).

Since SP is transferred during mating to females and enters the hemolymph (Haussmann et al. 2013), we wanted to test whether SPR is required in these neurons for inducing PMRs after mating. For *SPR RNAi* in *dsx ∩ fru11/12* and *SPR8 ∩ fru 11/12* neurons, no reduction, or a partial reduction, of receptivity was observed, respectively, while *SPR RNAi* in *dsx ∩ SPR8* neurons turned virgin females unreceptive (Figure 5A). Expression of mSP in *dsx ∩ fru11/12* neurons in the context of *SPR RNAi* partially reduced receptivity again suggesting additional receptors for SP (Haussmann et al. 2013).

Strikingly, however, *SPR RNAi* in these neurons prevented egg laying independent of whether SP was delivered by mating or when tethered to the membrane of these neurons (Figure 5B).

These results demonstrate that neurons identified by *split-GAL4* intersected expression of *SPR8* with *dsx* or *fru11/12*, or *fru11/12* with *dsx* are genuine SP targets as they rely on *SPR* and PMRs are induced by SP delivered through mating.

Expression of mSP in distinct neurons in the brain induces PMRs

The analysis of *ppkGAL4* neurons in SP-insensitive *Nup54* alleles revealed a hierarchy of trunk neurons that dominate over central brain neurons (Nallasivan et al. 2021). To focus on the role of central brain neurons, we generated a *UAS mSP* line with a stop cassette (*UAS FRTstopFRT mSP*) that allows to restrict expression of mSP to the head in the presence of *otdflp*, which only expresses in the head (Figure 6A), but not in the trunk (Asahina et al. 2014; Nallasivan et al. 2021).

In combination with the intersectional approach, we now can restrict mSP expression to few central brain neurons, or alternatively activate or silence these neurons (Figure 6B). Expression of mSP in *SPR8* ∩ *dsx*, *fru11/12* ∩ *dsx* or *SPR8* ∩ *fru11/12* neurons in the central brain significantly reduced receptivity, but oviposition was only substantially induced in *SPR8* ∩ *dsx* brain neurons (Figures 6C and 6D). In *fru11/12* ∩ *dsx* or *SPR8* ∩ *fru11/12*, PMR inducing neurons from the VNC could be required to potentiate the response.

These results clearly demonstrate a role for brain neurons in the SP response. However, we noticed that the flipase approach can result in false negatives as *fruflp* inserted in the same position in the endogenous locus as *fruGAL4* does not induce a response with *UAS FRTstopFRT* mSP in contrast to *fruGAL4* induced expression of mSP. In contrast, the same experiment with *dsxGAL4* and *dsxflp* results in a positive SP response indistinguishable from mated females (Haussmann et al. 2013).

Next, we tested whether neuronal activation or inhibition would induce a post-mating response. Strikingly, conditional activation of *SPR8* ∩ *dsx*, *fru11/12* ∩ *dsx* or *SPR8* ∩

fru11/12 brain neurons with TrpA1in adult females completely inhibited receptivity and induced egg laying comparable to mated females (Figures 6C and 6D). In contrast, inhibition of these neurons with tetanus toxin (TNT) did not alter the virgin state, e.g. receptivity was not reduced and egg laying was not induced (Figures 6C and 6D).

Genital tract neurons do not mediated changes in receptivity and oviposition by mSP

Since genital tract sensory neurons have been postulated to induce the SP response, we tested previously identified *split-GAL4* (*SPSN-1: VT058873 ∩ VT003280/FD6* and *SPSN-2: VT58873 ∩ VT033490*) lines, which upon neuronal inhibition reduced receptivity and induced egg laying (Feng et al. 2014), for their capacity to induce the SP response upon expression of mSP. Both lines reduced receptivity and induced egg laying upon expression of mSP (Figures S4A and S4B).

Expression analysis of these two lines revealed that in addition to expression in genital tract sensory neurons (Figures S4C, S4D, S4G and S4H), they also showed expression in the brain and ventral nerve cord (Figures S4K, S4L, S4O and S4P). Intriguingly, the brain neurons labeled in SPSN-1 resembled the neurons identified by *SPR8 ∩ FD6* (Figure 4G).

To determine whether SPSN neurons could overlap with expression of *SPR*, *dsx* and *fru* we analysed co-expression with *ocelliless* (*VT05573*), *Gyc76C* (*VT033490*) and *CG31637* (*FD6*), which are the genes where the enhancers of the *split-GAL4* lines originate, in the single cell brain atlas (Li et al. 2022). *CG31637* co-expressed in many cells with *SPR* and *fru*, but only few cells with *dsx* (Figures S6A-S6C). Expression of *ocelliless* with *SPR* and *fru* is broad, while only one neuron expressed with and *Gyc76C* in the brain (Figures S6D, S6E, S6G and S6H). Expression of *ocelliless* with *dsx* is restricted to two neurons, and no overlap was detected with *Gyc76C* in the brain Figures S6F-S6I).

When we analysed *split-GAL4* combinations of SPSN (VT058873, the common line in the SPSN1 and 2 lines) with *SPR8*, *fru11/12* and *dsx*, we observed full response to *mSP* expression for the intersection with *SPR8* and *fru11/12*, and a partial response for the *SPSN* ∩ *dsx* intersection (Figure S7A and S7B). Intriguingly, all of these *split-Gal4* combinations expressed in few neurons in the brain, the VNC and genital tract neurons except for *VY058873* ∩ *fru11/12* (Figure S7C-S7N).

We then restricted expression of mSP and induction of neuronal activity to the head with these splitGAL4 combinations using *FRTstop* casettes and *otdflp*. In this set up, we can induce PMRs from mSP expression or neuronal activation from TrpA1 expression with the *VY058873* ∩ *SPR8* and *dsx* combination, but not with the *fru11/12* combination (Suppl Fig S7O and S7P). For the VT058873 ∩fru11/12 intersection PMR inducing neurons likely reside in the VNC.

ppk neurons do not intersect with SPR, fru, dsx and FD6 neurons in inducing PMRs by mSP

Expression of *UASmSP* using a *GAL4* driven by a promoter fragment of the *ppk* gene can also induce PMRs (Figures S8A and S8B) (Hasemeyer et al. 2009; Yang et al. 2009). The complement of neurons labeled with *ppkGAL4* consists of at least two populations including prominently sensory neurons, but also eight interneurons in the central brain (Nallasivan et al. 2021). These brain neurons show severe developmental defects in SP-insensitive *Nup54* mutant alleles, but they receive inhibitory input from sensory neurons (Nallasivan et al. 2021).

To evaluate whether *ppkGAL4* neurons are part of the previously identified expression patterns, we intersected them by crossing *GAL4-AD* lines *SPR8*, *SPR12* and *fru11/12* and the pan-neural *nSybAD* with a *ppk GAL4-DBD* line containing the previously used 3 kb promoter

fragment (Grueber et al. 2003; Seidner et al. 2015; Riabinina et al. 2019). Surprisingly, none of these *split-GAL4* combinations reduced female receptivity or increased egg laying (Figures S8A and S8B, and Figures S8A and S8B).

Few GFP expressing neurons were detected in the brain for the *nSyb* ∩ *ppk* and the *fru11/12* ∩ *ppk* intersection (Figures S8C-S8F) or abdominal ganglion (Figures S8G-S8J). For the *nSyb* ∩ *ppk* and the *SPR8* ∩ *ppk* intersection we detected GFP expression in genital tract sensory neurons (Figures S8O and S8P), but not for the other combinations (Figures S8K and S8R).

Inhibiting or activating neurons with these split-Gal4 combinations did not reduce receptivity or induce egg laying (Figures S8L-S8O). How exactly *ppk* neurons labeled with *ppkGAL4* impact on PMRs, however, needs to be further evaluated in follow-up studies. Moreover, if genetical tract neurons were SP target sites, an SP response would have been expected for the *nSyb* ∩ *ppk* intersection, which we did not observe.

Female post-mating neuronal circuitry contains neurons that reduce receptivity without inducing oviposition in response to mSP

A number of additional *split-GAL4* combinations with restricted expression have been identified that play a role in female reproductive behaviors (Wang et al. 2020a; Wang et al. 2020b; Wang et al. 2021). These lines express in a subset of *dsx* expressing neurons (*pC1-SS1*), in oviposition descending neurons (*oviDN-SS1* and 2), in oviposition excitatory neurons (*oviEN-SS1* and 2), in oviposition inhibitory neurons (*oviIN-SS1* and 2), and in vaginal plate opening neurons (*vpoDN-SS1*, also termed ovipositor extrusion/rejection behavior neurons (Aigaki et al. 1991; Soller et al. 2006)). When we analyzed these lines for a response to mSP expression, receptivity was reduced from mSP expression in *oviEN-SS2*, *oviN-SS1* and

vpoDN-SS1 neurons, but no egg laying was induced from mSP expression in any of these neurons (Figure S9A and S9B).

In genital tract neurons, *OviDN-SS1s*, *OviEN-SS1*, *OviIN-SS1* and *vpoDNs* express, but *OviDN-SS1s* and *OviEN-SS1* express weakly (Figure S9C and S9J).

Interference of neuronal activity in SPRINz reveals regulatory hierarchy

Both inhibitory and activating neurons have been attributed to impact on PMRs (Kvitsiani and Dickson 2006; Yapici et al. 2008; Rezaval et al. 2012). These neurons seem to be part of intersecting circuitry as general inhibition of *ppkGAL4* neurons by tetanus toxin (TNT) only partially blocks the SP response in contrast to inhibition of *ppkGAL4* neurons in the brain alone (Nallasivan et al. 2021).

When we inhibited neuronal activity by expression of TNT (Sweeney et al. 1995), we observed a significant reduction of receptivity for all *split-Gal4* combinations, though only partially for inhibition in *fru11/12* ∩ *FD6* neurons. Likewise, all *split-Gal4* combinations induced a significant increase in egg laying (Figures S10A and S10B). Ablation of these neurons by expression of apoptosis inducing *reaper* and *hid* genes essentially replicated the results from neuronal inhibition indicating that SPR target neurons are modulatory and are not part of motor circuits because females laid eggs and performed normally in receptivity assays (Figures S10C and S10D).

To evaluate the composition of the intersected expression patters into inhibitory and activating neurons we also expressed the *Bacillus halodurans* sodium channel (NaChBac) (Feng et al. 2014) to activate all of the intersected neurons. Here, we found a significant reduction of receptivity for four of the five *split-GAL4* combinations, though only partially for activation of *SPR8* ∩ *dsx* neurons (Figure S10E). Activating *fru11/12* ∩ *FD6* neurons did not reduce receptivity (Figure S10E). Likewise, we found the same pattern for the induction

of egg laying (Figure S10F). Four of the five *split-GAL4* combinations induced a significant increase which was only partial in *SPR8* ∩ *dsx* neurons and no egg laying was induced by activating *fru11/12* ∩ *FD6* neurons.

Essentially, these results are consistent with previous findings that inhibitory neurons prevail (Nallasivan et al. 2021), possibly as input from trunk neurons as found for *ppk* expressing neurons.

mSP responsive neurons operate in higher order sensory processing in the brain

With the split-GAL4 approach we identified five distinct neuronal sub-types that can induce PMRs. To find out whether these neurons receive input from distinct entry points in the brain and to identify the target neurons of these mSP responsive neurons, we used the *retro*- and *trans*-Tango technique to specifically activate reporter gene expression in up- and down-stream neurons (Talay et al. 2017; Sorkaç et al. 2023)(Figures 7A-O).

In the brain, the *retro*-Tango analysis did not identify primary sensory neurons, but higher order neurons in the central brain in all five *split-GAL4* combinations (Fig 7A-E). In addition, neurons in the suboesophagal ganglion were marked from *SPR8* intersections with *dsx* and *FD6*, and in *dsx* ∩ *fru11/12*. In *dsx* ∩ *fru11/12*, neurons in the optic lobe (medulla) were marked. In addition, a strong signal was observed in all five *split-GAL4* combinations in the mushroom bodies (Figs 7A-E). Although mushroom bodies are dispensable for PMRs (Fleischmann et al. 2001) their connection to SP target neurons indicates an experience dependent component of PMRs .

The *trans*-Tango analysis identified a subset of neurons with cell bodies in the suboesophageal ganglion with projections to the *pars intercerebralis* for *SPR8* ∩ *dsx* and *fru11/12* ∩ *dsx* neurons (Figures 7K and 7L). For *SPR8* ∩ *fru11/12* and *SPR8* ∩ *FD6* neurons common target neurons were found in the antennal mechanosensory and motor centre

(AMMC) region with a single neuron identified near the mushroom body region (Figures 7M and 7N) (Ishimoto and Kamikouchi 2021). For *fru11/12* ∩ *FD6* no obvious targets were identified in the central brain (Figure 7O).

In the VNC, the *trans*-Tango analysis showed post-synaptic targets within the abdominal ganglion with all five *split-GAL4* combinations indicating an interconnected neuronal network (Figure S11A-S11O), which needs to be elaborated in detail. In the genital tract, no post-synaptic targets were detected indicating that these are afferent neurons integrating sensory input (Figure S11P-S11AD).

Taken together, circuitries identified via *retro*- and *trans*-Tango place SP target neurons at the interface of sensory processing interneurons connecting to two commonly shared post-synaptic processing neuronal populations in the brain. Hence, our data indicate that SP interferes with sensory input processing from multiple modalities that are canalized to higher order processing centres to generate a behavioural output.

Discussion

Much has been learned about the neuronal circuitry governing reproductive behaviors in *Drosophila* from interfering with neuronal activity in few neurons selected by intersectional expression using *split-GAL4* (Wang et al. 2020a; Wang et al. 2020b; Wang et al. 2021). However, how sex-peptide signaling as main inducer of the post-mating response, prominently consisting of refractoriness to re-mate and induction of egg laying, is integrated in this circuitry is not completely understood (Haussmann et al. 2013).

Here, we addressed this gap by identifying regulatory regions in *SPR*, *fru* and *dsx* genes driving membrane-tethered expression of SP in subsets of neurons to delineate SP targets to very few neurons in the central brain and the ventral nerve cord by intersectional expression. Consistent with previous analysis describing multiple pathways for the SP

response (Haussmann et al. 2013), we find five distinct populations of interneurons in the central brain directing PMRs. In SP target neurons in the central brain, SPR is essential to induce PMRs when receiving SP from males through mating. From mapping post-synaptic targets by *trans*-Tango, we identified two populations of interneurons. The architecture of this circuitry is reminiscent for processing of sensory input transmitted to central brain pattern generators for behavioral output. Hence, SP interferes at several levels for coordinating PMRs, but also leaves the female the opportunity to interfere under unfavorable conditions with specific elements of PMRs, e.g., if there is no egg laying substrate, females will still not remate (Haussmann et al. 2013). Likewise, mated females will not lay eggs despite suitable egg laying substrates if parasitoid wasps are present (Kacsoh et al. 2015). Thus, the architecture of female PMRs contrasts with male-courtship behavior consisting of a sequel of behavioral elements that once initiated will always follow stereotypically to the end culminating in mating, or start from the beginning when interrupted (Hall 1994; Greenspan and Ferveur 2000).

SP induces PMRs via entering the hemolymph to target neurons in the central brain and ventral nerve cord

Early characterization of the SP signaling cascade demonstrated induction of PMRs from various other sources than mating including transgenic secretion from the fat body, expression as membrane-tethered form on neurons or injection of synthetic peptide into the hemolymph (Chen et al. 1988; Aigaki et al. 1991; Schmidt et al. 1993; Nakayama et al. 1997). Likewise, SP is detected in the hemolymph after mating at a PMR inducing concentration (Haussmann et al. 2013). Moreover, PMRs are induced faster, when SP is injected compared to induction by mating (Haussmann et al. 2013). This delay, however, is not attributed to sperm binding of SP as it is unchanged after mating with spermless males.

These results suggest that SP reaches its targets through entering the circulatory system to target neurons and contrasts a previously proposed model favoring genital tract neurons as SP sensors from the lumen of the genital tract (Hasemeyer et al. 2009; Yang et al. 2009; Rezaval et al. 2012).

In further support of the internalization model, we identified *GAL4* drivers that express mSP in genital tract neurons, but do not induce PMRs. Also, *SPR12* does not express in genital tract neurons, but induces egg laying by expression of mSP. Moreover, expression of mSP predominantly in the trunk (including all genital tract sensory neurons), only induces egg laying, but does not change receptivity. Likewise, expression of mSP specifically in the brain (*SPR8* ∩ *dsx*) can reduce receptivity and induce egg laying indistinguishable from mated females.

A *ppkGAL4* line generated by P-element mediated transformation can induce PMRs by expression of *UAS mSP* (Grueber et al. 2003). The same promoter fragment fused to a *GAL4 DBD* and inserted by phiC31 integration into a landing site intersected with pan-neural *nSyb AD* line (Seidner et al. 2015; Riabinina et al. 2019), however, does not induce a SP response despite being expressed in genital tract neurons. We found that the *ppkGAL4* expresses in a few neurons in the brain and VNC (Nallasivan et al. 2021), but this expression is absent in *nSyb* ∩ *ppk* intersection. Likely, the *ppkGAL4* construct is inserted in a locus that contains an enhancer that drives expression in SP target neurons.

These results are in strong favor for SP entering the hemolymph to target neurons in the ventral nerve cord for inducing egg laying, and in the central brain for reducing receptivity and inducing egg laying (Haussmann et al. 2013).

Integration of SP signaling into the circuitry directing reproductive behaviours

Reduction of receptivity and induction of egg laying are both induced by the same critical concentration of injected SP (Schmidt et al. 1993; Haussmann et al. 2013) initially suggesting a simple on/off system for PMRs likely initiated from a small population of neurons. However, such model would not allow to split the SP response into individual PMR components by expression of mSP.

Here, we identified several *GAL4* drivers, that can induce only egg laying (*SPR12*, *FD3*, *FD4* and *tsh GAL4*), but do not reduce receptivity, and others that can only reduce receptivity (*oviEN-SS2*, *oviIN-SS1* and *vpoDN-SS1*), but do not induce egg laying. Strikingly *tshGAL4*, that expresses predominantly in the trunk only affects egg laying suggesting a role for the abdominal ganglion in egg laying. Moreover, all of the *split-GAL4* combinations affecting egg laying express in the abdominal ganglion and *dsx* neurons in the abdominal ganglion have been identified to induce egg laying (Rezaval et al. 2012; Zhou et al. 2014). Hence, this neuronal structure has a key role in regulating egg laying. Since more than a single neuronal population seems to direct egg laying, further high-resolution mapping is required to identify individual neuronal population within the abdominal ganglion (Jang et al. 2017; Oliveira-Ferreira et al. 2023).

Since *tshGAL4* only induces egg laying, neurons in the brain must direct reduction of receptivity. Through intersectional expression in combination with head-specific expression of *otdflp*, we could express mSP only in the brain by FLP mediated brain-specific excision of a stop cassette. We observed a significant reduction in receptivity for all five intersections tested, but for four the response is only partial likely due to the inefficiency of FLP mediated recombination.

Moreover, brain neurons can also induce egg laying when *SPR8* is intersected with *dsx*, and to some extent also from *SPR8* intersection with *fru11/12*. Due to the inefficiency of

480 FLP mediated recombination, however, this is likely an underestimate and solving this issue
481 requires development of more robust tools.

482 In any case, however, our results show that PMRs can be induced from mSP
483 expression from several sites suggesting interference with processing of sensory information
484 at the level of interneurons. In particular, *SPR8* ∩ *fru11/12* neurons resemble auditory
485 AMMC-B2 neurons involved in processing of information of the male love song (Yamada et
486 al. 2018). Likewise, *SPR8* ∩ *dsx* neurons seem to overlap with dimorphic *dsx* pCL2
487 interneurons that are part of the 26 neurons constituting the pC2 neuronal population
488 involved in courtship song sensing, mating acceptance and ovipositor extrusion for rejection
489 of courting males (Kimura et al. 2015; Deutsch et al. 2019; Wang et al. 2020a). The *SPR8* ∩
490 *FD6* neurons resemble dopaminergic *fru* P1 neurons involved in courtship and the *fru11/12* ∩
491 *dsx* neurons seem to overlap with *dsx* pCd and neuropeptide F neurons involved in courtship
492 (Zhang et al. 2021). In females, pC1d neurons have been linked to aggression (Deutsch et al.
493 2020; Schretter et al. 2020). The *fru11/12* ∩ *FD6* neurons resemble a class of gustatory
494 pheromone sensing neurons (Sakurai et al. 2013). Although we likely have not identified all
495 SP sensing neurons, our resources will provide a handle to future exploration of the details of
496 this neuronal circuitry incorporating SP signaling for inducing PMRs.

497

498 **Conclusions**

499 We have identified distinct SP sensing neurons in the central brain and the ventral
500 nerve cord. Since these five different SP sensing neuronal populations in the central brain
501 converge into two target sites, our data suggest a model (Figure 7P), whereby SP signaling
502 interferes with integration of sensory input. Independent interference with different sensory
503 modalities opts for the female to counteract male manipulation at the level of perception of

individual sensory cues to adapt to varying physiological and environmental conditions to maximize reproductive success.

Acknowledgments: We thank T. Aigaki, G. Barnea, P. Soba, W.J. Joiner, B. Dickson, S. Goodwin, C. Rezaval, D. Anderson, J.J. Hodge, A. Hidalgo, S. Collier, O. Raibinina, the Bloomington stock center, the Vienna Drosophila RNAi Center for flies, T. Aigaki and W.J. Joiner for plasmids, the University of Cambridge Department of Genetics Fly Facility and FlyORF for injections, D. Scocchia for help with PCR and, I.U. Haussmann, Y.J. Kim, J.C. Billeter and J-R Martin for comments on the manuscript. We acknowledge funding by the Biotechnology and Biological Science Research Council to MS.

Author contributions: MS conceived and directed the project. MPN performed genetic experiments and imaging. MS and SS performed genetic and DS imaging experiments. MPN and MS analyzed data. MS wrote the manuscript with support from MPN. All authors read and approved the final manuscript.

Data availability: Brain and VNC images for splitGal4 combinations of SP Response Inducing Neurons have been deposited in Virtual Fly Brain and will be published under the following accession numbers: VFB_x0000000-9. All data generated or analysed during this study are included in the paper and supplementary files; source data files are provided for all figures.

Declarations

Ethics approval and consent to participate: Not applicable.

Consent for publication: Not applicable.

Competing interests: The authors declare no competing interests.

Materials and methods

Key resources table

REAGENT or RESOURCE	SOURCE	IDENTIFIER
Antibodies		
Anti-HA (rat, 3F10)	Roche	
Anti-GFP (rabbit)	Molecular Probes	
Goat anti-rabbit Alexa Fluor 488	Molecular Probes	
Goat anti-rabbit Alexa Fluor 546	Molecular Probes	
Goat anti-rabbit Alexa Fluor 647	Molecular Probes	
Goat anti-rat Alexa Fluor 647	Molecular Probes	
Bacterial and Virus Strains		
For recombinant DNA cloning: *Escherichia coli*: DH5α	New England Biolabs	
Experimental Models: Organisms/Strains		
Drosophila: wild-type: Canton S	Soller lab	
Drosophila: w*; UASmSP (3rd, 61C)	T. Aigaki	
Drosophila: dsx-GAL4 inserted into the endogenous dsx gene (84E5-84E6)	S. Goodwin	
Drosophila: fru-GAL4 inserted into the endogenous fru gene (91A6-91B3) *Drosophila*: nSyb GAL4 (3rd)	B. Dickson S. Goodwin	
Drosophila: ppk-GAL4/CyO	Bloomington Stock Centre	BDSC 49021
Drosophila: tshGAL4-1/CyO	Bloomington Stock Centre	BDSC 3040
elav FRTstopFRT GAL4	Soller lab	
otdflp	D. Anderson	
UASmCD8GFP (X)	Bloomington Stock Centre	BDSC 5136
UASmCD8GFP (2nd)	Bloomington Stock Centre	BDSC 5137
UAS-H2B::YFP (2nd)	A. Hidalgo	
elavLexA (2nd)	Bloomington Stock Centre	BDSC 52676
LexAop NLStomato (2nd)	Bloomington Stock Centre	BDSC 66690
UAS TNT (2nd)	J.J. Hodge	
UAS TrpA1 (3rd)	Bloomington Stock Centre	BDSC 26264
UASFlybow 1.1 (myrGFP, 2nd)	Bloomington Stock Centre	BDSC 35537
UAS-NaCh::BacGFP (3rd)	Bloomington Stock Centre	BDSC9467

UAS Reaper/FM7;UAS Hid/CyO	Bloomington Stock Centre	BDSC 5823 BDSC65403
UAS FRTstopFRT GFP/CyO UAS FRTstopFRT TNT/CyO	B. Dickson B. Dickson	
UAS FRTstopFRT TrpA1/CyO	B. Dickson	
UAS FRTstopFRT mSP (3rd)	This study	
UAS dicer2; UAS SPR RNAi (X, 3rd)	B. Dickson	
SPR	Bloomington Stock Centre	BDSC 7708
Df(1)JC70/FM7c	Bloomington Stock Centre	BDSC 944
Drosophila: nSyb p65-GAL4.AD (attP40)	O. Riabinina	
Drosophila SPR8 AD: VT057286-p65.AD (attP40)	Bloomington Stock Centre	BDSC71392
Drosophila Fru11/12 AD: VT043695-p65.AD (attP40)	Bloomington Stock Centre	BDSC72065
Drosophila dsx DBD	S. Goodwin	
Drosophila dsx24 DBD: R42G02-GAL4.DBD (attP2)	Bloomington Stock Centre	
Drosophila SPR8 DBD: VT057286-Gal4.DBD (attP2)	Bloomington Stock Centre	BDSC71425
Drosophila fru11/12 DBD: VT043695-GAL4.DBD (attP2)	Bloomington Stock Centre	BDSC72788
Drosophila FD6 DBD: VT003280-GAL4.DBD (attP2)	Bloomington Stock Centre	BDSC75877
Drosophila ppk DBD: ppk-GAL4.DBD (VK00027, 89E11)	W. J. Joiner	
Drosophila SPR12 AD: VT057292-p65.AD (attP40)	Bloomington Stock Centre	BDSC72924
UAS-myrGFP QUAS-mtdTomato-3xHA; trans-Tango	Bloomington Stock Centre	BDSC 95317
QUAS-mtdTomato-3xHA; retro-Tango	G. Barnea	
Drosophila: fru1 GAL4: R23C03-GAL4 (attP2)	Bloomington Stock Centre	BDSC 49021
Drosophila: fru2 GAL4, R22H11-GAL4 (attP2)	Bloomington Stock Centre	BDSC 48043
Drosophila: fru3 GAL4, R21H09-GAL4 (attP2)	Bloomington Stock Centre	BDSC 49867
Drosophila: fru4 GAL4, R23C12-GAL4 (attP2)	Bloomington Stock Centre	BDSC 49026
Drosophila: fru5 GAL4, R22F06-GAL4 (attP2)		KDRC 11848
Drosophila: fru6 GAL4, R23D03GAL4	Bloomington Stock Centre	N/A
Drosophila: fru7 GAL4, R22B09-GAL4	Bloomington Stock Centre	N/A
Drosophila: fru8 GAL4, R23B12-GAL4 (attP2)	Korea Drosophila Resource Centre	KDRC 11849
Drosophila: fru9 GAL4, R22A02-GAL4 (attP2)	Bloomington Stock Centre	BDSC 49868
Drosophila: fru10 GAL4, R22C05-GAL4 (attP2)	Bloomington Stock Centre	BDSC 49301

Drosophila: fru11 GAL4, R22C11-lexA (attP40)	Bloomington Stock Centre	BDSC 52604
Drosophila: fru12 GAL4, R22A11-GAL4 (attP2)	Bloomington Stock Centre	BDSC 48966
Drosophila: fru13 GAL4, R23A06-GAL4 (attP2)	Bloomington Stock Centre	BDSC 49009
Drosophila: fru14 GAL4, R22C03-GAL4 (attP2)	Korea Drosophila Resource Centre	KDRC 11868
Drosophila: fru15 GAL4, R23B04-GAL4 (attP2)	Bloomington Stock Centre	BDSC 49016
Drosophila: fru16 GAL4, R22C07-GAL4 (attP2)	Bloomington Stock Centre	BDSC 48975
Drosophila: fru17 GAL4, R23C08-GAL4 (attP2)	Korea Drosophila Resource Centre	KDRC 11835
Drosophila: fru18 GAL4, R23C07GAL4	Bloomington Stock Centre	N/A
Drosophila: fru19 GAL4, R22B10-GAL4 (attP2)	Bloomington Stock Centre	BDSC 48969
Drosophila: fru20 GAL4, R22E10-GAL4 (attP2)	Bloomington Stock Centre	BDSC 49302
Drosophila: fru21 GAL4, R22D11-GAL4 (attP2)	Bloomington Stock Centre	BDSC 48982
Drosophila: fru22 GAL4, R22H07-GAL4 (attP2)	Bloomington Stock Centre	BDSC 490003
Drosophila: fru23 GAL4, R21H02-GAL4 (attP2)	Korea Drosophila Resource Centre	KDRC 11847
Drosophila: fru24 GAL4, R23B11-GAL4 (attP2)	Bloomington Stock Centre	BDSC 49019
Drosophila: fru25 GAL4: VT043674-GAL4 (attP2)	Bloomington Stock Centre	N/A
Drosophila: fru26 GAL4, VT043675-GAL4 (attP2)	Bloomington Stock Centre	N/A
Drosophila: fru27 GAL4, VT043676-GAL4 (attP2)	Bloomington Stock Centre	N/A
Drosophila: dsx1 GAL4, R39E06-GAL4 (attP2)	Bloomington Stock Centre	BDSC 50051
Drosophila: dsx2 GAL4, R40A05-GAL4 (attP2)	Bloomington Stock Centre	BDSC 48138
Drosophila: dsx3 GAL4, R40F03-GAL4 (attP2)	Bloomington Stock Centre	BDSC 47355
Drosophila: dsx4 GAL4, R40F04-GAL4	Bloomington Stock Centre	N/A
Drosophila: dsx5 GAL4, R41A01-GAL4	Bloomington Stock Centre	N/A
Drosophila: dsx6 GAL4, R41D01GAL4	Bloomington Stock Centre	N/A
Drosophila: dsx7 GAL4, R41F06-GAL4 (attP2)	Bloomington Stock Centre	BDSC 47584
Drosophila: dsx8 GAL4, R42C06-GAL4 (attP2)	Bloomington Stock Centre	BDSC 50150
Drosophila: dsx9 GAL4, R42D02-GAL4 (attP2)	Bloomington Stock Centre	BDSC 41250
Drosophila: dsx10 GAL4, R42D04-GAL4 (attP2)	Bloomington Stock Centre	BDSC 47588
Drosophila: dsx11 GAL4, VT038171-GAL4 (attP2)	Bloomington Stock Centre	N/A
Drosophila: dsx12 GAL4, VT038169-GAL4 (attP2)	Bloomington Stock Centre	N/A
Drosophila: dsx13 GAL4, VT038167-GAL4 (attP2)	Bloomington Stock Centre	N/A

Drosophila: dsx14 GAL4, VT038166-GAL4 (attP2)	Bloomington Stock Centre	N/A
Drosophila: dsx15 GAL4, VT038161-GAL4 (attP2)	Bloomington Stock Centre	N/A
Drosophila: dsx16 GAL4, VT038159-GAL4 (attP2)	Bloomington Stock Centre	N/A
Drosophila: dsx17 GAL4, VT038157-GAL4 (attP2)	Bloomington Stock Centre	N/A
Drosophila: dsx18 GAL4, VT038155-GAL4 (attP2)	Bloomington Stock Centre	N/A
Drosophila: dsx19 GAL4, VT038151-GAL4	Bloomington Stock Centre	N/A
Drosophila: dsx20 GAL4, VT038149-GAL4 (attP2)	Bloomington Stock Centre	N/A
Drosophila: dsx21 GAL4, P{VT038148-GAL4 (attP2)	Bloomington Stock Centre	N/A
Drosophila: dsx22 GAL4, P{VT038147-GAL4 (attP2)	Bloomington Stock Centre	N/A
Drosophila: dsx23 GAL4, R22H07-GAL4 (attP2)	Bloomington Stock Centre	N/A
Drosophila: dsx24 GAL4, R21H02-GAL4 (attP2)	Bloomington Stock Centre	N/A
Drosophila: dsx25 GAL4, R21B01-GAL4 (attP2)	Bloomington Stock Centre	N/A
Drosophila: SPR1 GAL4, R78F09-GAL4	Bloomington Stock Centre	N/A
Drosophila: SPR2 GAL4, R78F11-GAL4	Bloomington Stock Centre	N/A
Drosophila: SPR3 GAL4, R78E11-GAL4	Bloomington Stock Centre	N/A
Drosophila: SPR4 GAL4, R78E12-GAL4 (attP2)	Bloomington Stock Centre	BDSC 40002
Drosophila: SPR5 GAL4, R78G09-GAL4 (attP2)	Bloomington Stock Centre	BDSC 40015
Drosophila: SPR6 GAL4, R78G08-GAL4	Bloomington Stock Centre	N/A
Drosophila: SPR7 GAL4, R78F07-GAL4 (attP2)	Bloomington Stock Centre	BDSC 47409
Drosophila: SPR8 GAL4, R78F10-GAL4 (attP2)	Bloomington Stock Centre	BDSC 40007
Drosophila: SPR9 GAL4, R78G02-GAL4 (attP2)	Bloomington Stock Centre	BDSC 40010
Drosophila: SPR10 GAL4, R78G07-GAL4	Bloomington Stock Centre	N/A
Drosophila: SPR11 GAL4, R78G04-GAL4 (attP2)	Bloomington Stock Centre	BDSC 40012
Drosophila: SPR12 GAL4, R78F05-GAL4	Bloomington Stock Centre	N/A
Drosophila: SPR13 GAL4, R78G05-GAL4 (attP2)	Bloomington Stock Centre	BDSC 41308
Drosophila: SPR14 GAL4, R78G06-GAL4	Bloomington Stock Centre	N/A
Drosophila: SPR15 GAL4, R78G03-GAL4 (attP2)	Bloomington Stock Centre	BDSC 40011
Drosophila: SPR16 GAL4, R78F06-GAL4	Bloomington Stock Centre	N/A
Drosophila: SPR17 GAL4, R78F12-GAL4	Bloomington Stock Centre	N/A

Drosophila: SPR18 GAL4, R78F03-GAL4	Bloomington Stock Centre	N/A
Drosophila: SPR19 GAL4, R78F01-GAL4 (attP2)	Bloomington Stock Centre	BDSC 40003
Drosophila: SPR20 GAL4, R78G01-GAL4 (attP2)	Bloomington Stock Centre	BDSC 40009
Drosophila: SPR21 GAL4, R78F02-GAL4 (attP2)	Bloomington Stock Centre	N/A
Drosophila: SPR22 GAL4, R78F08-GAL4 (attP2)	Bloomington Stock Centre	N/A
Drosophila: FD1 GAL4, VT050405-GAL4 (attP2)	Vienna Drosophila Stock Centre	VDSC
Drosophila: FD2 GAL4, VT007068-GAL4 (attP2)	Vienna Drosophila Stock Centre	VDSC
Drosophila: FD3 GAL4, VT045154-GAL4 (attP2),	Vienna Drosophila Stock Centre	VDSC
Drosophila: FD4 GAL4, VT000454-GAL4 (attP2)	Vienna Drosophila Stock Centre	VDSC
Drosophila: FD5 GAL4, VT050247-GAL4 (attP2)	Vienna Drosophila Stock Centre	VDSC
Drosophila: FD6 GAL4, VT003280-GAL4 (attP2)	Vienna Drosophila Stock Centre	VDSC
Drosophila: SPR8 GAL4, R78F10-GAL4 (attP2);	Bloomington Stock Centre	BDSC 40007
Drosophila: SPR8 AD [VT057286-p65.AD (attP40)]; fru11/12 DBD [VT043695-GAL4.DBD (attP2)]	This study	Soller Lab
Drosophila: Fru11/12 AD [VT043695-p65.AD (attP40)]; FD6 DBD [VT003280-GAL4.DBD (attP2)]	This study	Soller Lab
Drosophila: SPR8 AD [VT057286-p65.AD (attP40)]; FD6 DBD [VT003280-GAL4.DBD (attP2)]	This study	Soller Lab
Drosophila: SPR8 AD [VT057286-p65.AD (attP40)]; dsx DBD (attP2)	This study	Soller Lab
Drosophila: Fru11/12 AD [VT043695-p65.AD (attP40)]; dsx DBD (attP2)	This study	Soller Lab
Drosophila: VT058873-GAL4.AD (attP40); SPR8 DBD [VT057286-GAL4.DBD(attP2)]	This study	Soller Lab
Drosophila: VT058873-GAL4.AD (attP40); Fru11/12 DBD [VT043696-GAL4.DBD(attP2)]	This study	Soller Lab
Drosophila: VT058873-GAL4.AD (attP40); dsx DBD (attp2)	This study	Soller Lab
Drosophila: nSyb p65-GAL4.AD (attp40); ppk DBD: ppk-GAL4.DBD [VK00027, 89E11]	This study	Soller Lab
Drosophila: SAG1, VT050405-GAL4.AD (attP40); VT007068-GAL4.DBD (attP2)	Bloomington Stock Centre	BDSC 66875
Drosophila: pC1-SS1, VT2002064-GAL4.AD (attP40); VT008469-GAL4.DBD (attP2)	Bloomington Stock Centre	BDSC 86830
Drosophila: oviDN-SS1, VT050660-GAL4.AD (attP40); VT028160-GAL4.DBD (attP2)	Bloomington Stock Centre	BDSC 86832
Drosophila: oviDN-SS2, VT026873-GAL4.AD (attP40); VT040574-GAL4.DBD (attP2)	Bloomington Stock Centre	BDSC 86831
Drosophila: oviEN-SS1, VT043086-GAL4.AD (attP40); VT034612-GAL4.DBD (attP2)	Bloomington Stock Centre	BDSC 86839
Drosophila: oviEN-SS2, VT034612-GAL4.AD (attP40); VT050229-GAL4.DBD (attP2)	Bloomington Stock Centre	BDSC 86833

Drosophila: oviIN-SS1, R68A10-GAL4.AD (attP40); VT010054-GAL4.DBD (attP2)	Bloomington Stock Centre	BDSC 86837
Drosophila: oviIN-SS2, VT026347-GAL4.AD (attP40); VT026035-GAL4.DBD (attP2)	Bloomington Stock Centre	BDSC 86838
Drosophila: vpoDN-SS1, R31D07-GAL4.AD (attP40); R52F12-GAL4.DBD (attP2)	Bloomington Stock Centre	BDSC 86868
Drosophila: SPSN1, VT058873-GAL4.AD (attP40); VT003280-GAL4.DBD (attP2)	Bloomington Stock Centre	BDSC 86834
Drosophila: SPSN2, VT058873-GAL4.AD (attP40); VT033490-GAL4.DBD (attP2)	Bloomington Stock Centre	BDSC 86870
Drosophila: SAG1, VT050405-GAL4.AD (attP40); VT007068-GAL4.DBD (attP2)	Bloomington Stock Centre	BDSC 66875
pUAST-GGTmSP FRTGFPstopFRT gBlock (FRT underlined) GAATTGGGAATTCGTTAACAGATCTGCGATCGCGG CCCGGGGATCTTGAAGTTCCTATTCCGAAGTTCCTA TTCTCTAGAAAGTATAGGAACTTCAGAGCGCTTTTG AAGCTAGCTAAAGAGCCTGCTAAAGCAAAAAAGAAG TCACCATGGTGTCGAGCGCAAGCAAGGGCGAGGA GCTGTTCACCGGGGTGGTGCCCATCCTGGTCGAGC TGGACGGCGACGTAAACGGCCACAAGTTCAGCGTG TCCGGCGAGGGCGAGGGCGATGCCACCTACGGCA AGCTGACCCTGAAGTTCATCTGCACCACCGGCAAG CTGCCCGTGCCCTGGCCCACCCTCGTGACCACCCT GACCTACGGCGTGCAGTGCTTCAGCCGCTACCCCG ACCACATGAAGCAGCACGACTTCTTCAAGTCCGCCA TGCCCGAAGGCTACGTCCAGGAGCGCACCATCTTC TTCAAGGACGACGGCAACTACAAGACCCGCGCCGA GGTGAAGTTCGAGGGCGACACCCTGGTGAACCGCA TCGAGCTGAAGGGCATCGACTTCAAGGAGGACGGC AACATCCTGGGGCACAAGCTGGAGTACAACTACAA CAGCCACAACGTCTATATCATGGCCGACAAGCAGA AGAACGGCATCAAGGTGAACTTCAAGATCCGCCAC AACATCGAGGACGGCAGCGTGCAGCTCGCCGACCA CTACCAGCAGAACACCCCCATCGGCGACGGCCCCG TGCTGCTGCCCGACAACCACTACCTGAGCACCCAG TCCGCCCTGAGCAAAGACCCCAACGAGAAGCGCGA TCACATGGTCCTGCTGGAGTTCGTGACCGCCGCCG GGATCACTCTCGGCATGGACGAGCTGTACAAGTAC TCAGATCTTTGCAAGCTTGTAGAGTTTCCCATTTAAT AATTCATATTATCTCGAATCTAGTCAATTACGGCTTT CCTCAAATAGAAAAATAAAAAAAATGAAAAAATGCAC TTGCCATTTAAACTTAGACGCGATAACGAATTCCGG GGATCTTGAAGTTCCTATTCCGAAGTTCCTATTCTCT AGAAAGTATAGGAACTTCAGAGCGCTTTTGAAGCTG CGGCCGCGGCTCGACGGTATCGATAAGCTTG	IDT	

534

535 **Fly strains and husbandry**

536 Flies were kept on standard cornmeal-agar food (1%industrial-grade agar, 2.1% dried
537 yeast, 8.6% dextrose, 9.7% cornmeal and 0.25% Nipagin, all in (w/v)) in a 12 h light : 12 h
538 dark cycle. Propionic acid was omitted from fly food as acidity affects egg laying (Gou et al.
539 2014). Genetic crosses were done in vials and kept at low density to ensure larvae were not

competing for food and if necessary, additional live yeast was added. For all behavioral assays, virgin and mated Canton-S were used as controls. Virgin females, e.g. from crosses of *GAL4* with *UASmSP*, were collected after emergence within a 5 h window and well-fed with live yeast sprinkled on food for maximum egg production and allowed to sexually mature (3–5 days).

To recombine 2nd chromosome inserts for *splitGAL4AD* (*attP40*) and 3rd chromosome *splitGAL4DBD* (*attP2*), standard genetic crossing schemes were used and final stocks were balanced with CyO and TM3 Sb (combined from from ST and CT stock, see key resource list). *SplitGal4AD* and *DBD* combination lines were then crossed to *UASmSP*. For meiotic recombination, final stocks were validated by behavioral analysis for *UAS mSP*, for *flp* with *eFeG UASCD8GFP* to monitor GFP expression and for *otdflp UASstopTrpA* and *otdflp UASstopTNT* by crossing to *elavGAL4* and monitored by lethality.

For enhanced recombination with *flp*, virgin females were transferred to 30º C after eclosion and kept for 5 d at this temperature before performing the behavioral assays. For induction of neuronal activity by temperature sensitive TrpA1, females were kept at 30º C.

To make *UAS FRTstopFRT mSP*, a gBlock (IDT) stop cassette with the FRT sequences used in the eFeG plasmid (Haussmann et al. 2008) was inserted into NotI cut *pUAST-GGTmSP* (gift from T. Aigaki) by Gibson assembly. In the stop-cassette, the *FRT* sequence is followed by a *GFP* with a 3'UTR from *ewg* containing polyA site 1 from intron 6 (Haussmann et al. 2011). Flies were transformed by *P*-element mediated transgenesis and a inserts on each chromosome were established that show a robust post-mating response with *dsxflp* indistinguishable from mated females.

Behavioral analysis

Females were examined for the main post-mating behaviors receptivity and oviposition as described previously and as follows (Soller et al. 1999; Soller et al. 2006). To generate mated females, one female and three males were added to fly vials and observed until mating and males were removed after mating. For receptivity tests, mature virgin or mated females were added to fly vials (95 mm length and 24 mm diameter) containing Canton S males with an aspirator and observed for 1 h, generally 3 females and 7 males. For these experiments, males were separated from females at least one day before the experiment. Receptivity tests were done in the afternoon with virgins, or 5-24 h after mating for controls. For oviposition, females were placed individually in fly vials in the afternoon and the number of eggs laid was counted the next day.

Statistical analysis

Sample size was based on previous studies, non-blinded and not pre-determined by statistical methods (Soller et al. 1997; Haussmann et al. 2013; Nallasivan et al. 2021). Behavioral data are representatives of at least three replicates that were performed on three different days. Statistical analysis of behavioral experiments were performed using GraphPadPrism 9 (GraphPad by Dotmatics) using one way Anova followed by pairwise comparisons with Tukey's test.

Immunohistochemistry and imaging

For the analysis of adult neuronal projection from *UAS CD8GFP, UAS H2BYFP,UASmyrGFP, lexAopNLStomato* or *QUAS mtdtomato3xHA* expressing brains, ventral nerve cords or genital tracts, tissues were dissected in PBS (137 mM NaCl, 10 mM phosphate, 2.7 mM KCl, pH7.4), fixed in 4% (w/v in PBS) paraformaldehyde for 15 minutes, washed three times in PBST (PBS with 1% BSA and 0.3% Triton-X100), then once in PBS

589 for 10 mins, mounted in Vectashield (Vector Labs) and visualized with confocal microscopy
590 using a Leica TCS SP8. If signals were weak, antibody *in-situ* stainings were done as
591 described previously (Haussmann et al. 2008) for validation using rat anti-HA (MAb 3F10,
592 1:20; Roche), rabbit anti-GFP (Molecular Probes, 1:100) and visualized with Alexa Fluor 488
593 (1:250; Molecular Probes or Invitrogen), Alexa Fluor 546 (1:250; Molecular Probes or
594 Invitrogen) or Alexa Fluor 647 (1:250; Molecular Probes or Invitrogen). For imaging, tissues
595 were mounted in Vectashield (Vector Labs).
596

597 **Confocal microscopy and image processing**

598 Adult tissues were scanned using a Leica SP8 confocal microscope equipped with a
599 set of fluorescent filters and hybrid detector (HyD). Adult brains were scanned using a 40x
600 HC PL APO 40x/1.30 lens with oil, 1024 x 1024 resolution and 0.96 µm Z-step. VNC and
601 genital tracts were scanned using a HC PL APO CS2 20X/0.75 with oil, 1024 x 1024
602 resolution and 0.96 µm Z-step. Images were obtained using Leica Application Suite X (LAS
603 X) imaging acquisition software. Raw data files were in LIF format and were processed using
604 FIJI.
605 For high resolution mapping neurons were identified in the virtual fly brain based on
606 registered *GAL4* expression and traces retrieved for modelling (Scheffer et al. 2020; Phelps et
607 al. 2021; Galili et al. 2022).
608

609 **References**

610 Aigaki T, Fleischmann I, Chen PS, Kubli E. 1991. Ectopic expression of sex peptide alters reproductive
611 behavior of female *D. melanogaster*. *Neuron* **7**: 557-563.
612 Anderson DJ. 2016. Circuit modules linking internal states and social behaviour in flies and mice. *Nat Rev*
613 *Neurosci* **17**: 692-704.
614 Aranha MM, Vasconcelos ML. 2018. Deciphering Drosophila female innate behaviors. *Curr Opin Neurobiol*
615 **52**: 139-148.
616 Asahina K, Watanabe K, Duistermars BJ, Hoopfer E, Gonzalez CR, Eyjolfsdottir EA, Perona P, Anderson DJ.
617 2014. Tachykinin-expressing neurons control male-specific aggressive arousal in Drosophila. *Cell* **156**:
618 221-235.

Avila FW, Ravi Ram K, Bloch Qazi MC, Wolfner MF. 2010. Sex peptide is required for the efficient release of stored sperm in mated Drosophila females. *Genetics* **186**: 595-600.

Avila FW, Sirot LK, LaFlamme BA, Rubinstein CD, Wolfner MF. 2011. Insect seminal fluid proteins: identification and function. *Annu Rev Entomol* **56**: 21-40.

Billeter JC, Rideout EJ, Dornan AJ, Goodwin SF. 2006. Control of male sexual behavior in Drosophila by the sex determination pathway. *Curr Biol* **16**: R766-776.

Carvalho GB, Kapahi P, Anderson DJ, Benzer S. 2006. Allocrine modulation of feeding behavior by the Sex Peptide of Drosophila. *Curr Biol* **16**: 692-696.

Chen PS, Stumm-Zollinger E, Aigaki T, Balmer J, Bienz M, Bohlen P. 1988. A male accessory gland peptide that regulates reproductive behavior of female D. melanogaster. *Cell* **54**: 291-298.

Cognigni P, Bailey AP, Miguel-Aliaga I. 2011. Enteric neurons and systemic signals couple nutritional and reproductive status with intestinal homeostasis. *Cell Metab* **13**: 92-104.

Cury KM, Axel R. 2023. Flexible neural control of transition points within the egg-laying behavioral sequence in Drosophila. *Nat Neurosci* **26**: 1054-1067.

Demir E, Dickson BJ. 2005. fruitless splicing specifies male courtship behavior in Drosophila. *Cell* **121**: 785-794.

Deutsch D, Clemens J, Thiberge SY, Guan G, Murthy M. 2019. Shared Song Detector Neurons in Drosophila Male and Female Brains Drive Sex-Specific Behaviors. *Curr Biol* **29**: 3200-3215.e3205.

Deutsch D, Pacheco D, Encarnacion-Rivera L, Pereira T, Fathy R, Clemens J, Girardin C, Calhoun A, Ireland E, Burke A et al. 2020. The neural basis for a persistent internal state in Drosophila females. *Elife* **9**.

Domanitskaya EV, Liu H, Chen S, Kubli E. 2007. The hydroxyproline motif of male sex peptide elicits the innate immune response in Drosophila females. *FEBS J* **274**: 5659-5668.

Dulac C, Kimchi T. 2007. Neural mechanisms underlying sex-specific behaviors in vertebrates. *Curr Opin Neurobiol* **17**: 675-683.

Feng K, Palfreyman MT, Hasemeyer M, Talsma A, Dickson BJ. 2014. Ascending SAG neurons control sexual receptivity of Drosophila females. *Neuron* **83**: 135-148.

Fleischmann I, Cotton B, Choffat Y, Spengler M, Kubli E. 2001. Mushroom bodies and post-mating behaviors of Drosophila melanogaster females. *J Neurogenet* **15**: 117-144.

Galili DS, Jefferis GS, Costa M. 2022. Connectomics and the neural basis of behaviour. *Current opinion in insect science* **54**: 100968.

Gou B, Liu Y, Guntur AR, Stern U, Yang CH. 2014. Mechanosensitive neurons on the internal reproductive tract contribute to egg-laying-induced acetic acid attraction in Drosophila. *Cell reports* **9**: 522-530.

Greenspan RJ, Ferveur JF. 2000. Courtship in Drosophila. *Annual review of genetics* **34**: 205-232.

Grueber WB, Ye B, Moore AW, Jan LY, Jan YN. 2003. Dendrites of distinct classes of Drosophila sensory neurons show different capacities for homotypic repulsion. *Curr Biol* **13**: 618-626.

Hall JC. 1994. The mating of a fly. *Science* **264**: 1702-1714.

Hasemeyer M, Yapici N, Heberlein U, Dickson BJ. 2009. Sensory neurons in the Drosophila genital tract regulate female reproductive behavior. *Neuron* **61**: 511-518.

Haussmann IU, Hemani Y, Wijesekera T, Dauwalder B, Soller M. 2013. Multiple pathways mediate the sex-peptide-regulated switch in female Drosophila reproductive behaviours. *Proc Biol Sci* **280**: 20131938.

Haussmann IU, Li M, Soller M. 2011. ELAV-mediated 3'-end processing of ewg transcripts is evolutionarily conserved despite sequence degeneration of the ELAV-binding site. *Genetics* **189**: 97-107.

Haussmann IU, White K, Soller M. 2008. Erect wing regulates synaptic growth in Drosophila by integration of multiple signaling pathways. *Genome Biol* **9**: R73.

Hopkins BR, Perry JC. 2022. The evolution of sex peptide: sexual conflict, cooperation, and coevolution. *Biological reviews of the Cambridge Philosophical Society* **97**: 1426-1448.

Isaac RE, Li C, Leedale AE, Shirras AD. 2010. Drosophila male sex peptide inhibits siesta sleep and promotes locomotor activity in the post-mated female. *Proc Biol Sci* **277**: 65-70.

Ishimoto H, Kamikouchi A. 2021. Molecular and neural mechanisms regulating sexual motivation of virgin female Drosophila. *Cell Mol Life Sci* **78**: 4805-4819.

Jang YH, Chae HS, Kim YJ. 2017. Female-specific myoinhibitory peptide neurons regulate mating receptivity in Drosophila melanogaster. *Nature communications* **8**: 1630.

Jenett A, Rubin GM, Ngo TT, Shepherd D, Murphy C, Dionne H, Pfeiffer BD, Cavallaro A, Hall D, Jeter J et al. 2012. A GAL4-driver line resource for Drosophila neurobiology. *Cell reports* **2**: 991-1001.

Kacsoh BZ, Bozler J, Ramaswami M, Bosco G. 2015. Social communication of predator-induced changes in Drosophila behavior and germ line physiology. *Elife* **4**.

Kim SJ, Lee KM, Park SH, Yang T, Song I, Rai F, Hoshino R, Yun M, Zhang C, Kim JI et al. 2024. A sexually transmitted sugar orchestrates reproductive responses to nutritional stress. *Nature communications* **15**: 8477.

Kim YJ, Bartalska K, Audsley N, Yamanaka N, Yapici N, Lee JY, Kim YC, Markovic M, Isaac E, Tanaka Y et al. 2010. MIPs are ancestral ligands for the sex peptide receptor. *Proc Natl Acad Sci U S A* **107**: 6520-6525.

Kimura K, Sato C, Koganezawa M, Yamamoto D. 2015. Drosophila ovipositor extension in mating behavior and egg deposition involves distinct sets of brain interneurons. *PLoS One* **10**: e0126445.

Kubli E. 1992. The sex-peptide. *Bioessays* **14**: 779-784.

Kvitsiani D, Dickson BJ. 2006. Shared neural circuitry for female and male sexual behaviours in Drosophila. *Curr Biol* **16**: R355-356.

Kvon EZ, Kazmar T, Stampfel G, Yáñez-Cuna JO, Pagani M, Schernhuber K, Dickson BJ, Stark A. 2014. Genome-scale functional characterization of Drosophila developmental enhancers in vivo. *Nature* **512**: 91-95.

Li H Janssens J De Waegeneer M Kolluru SS Davie K Gardeux V Saelens W David FPA Brbić M Spanier K et al. 2022. Fly Cell Atlas: A single-nucleus transcriptomic atlas of the adult fruit fly. *Science* **375**: eabk2432.

Luan H, Peabody NC, Vinson CR, White BH. 2006. Refined spatial manipulation of neuronal function by combinatorial restriction of transgene expression. *Neuron* **52**: 425-436.

Manning A. 1967. The control of sexual receptivity in female Drosophila. *Animal Behaviour* **15**: 239-250.

Manoli DS, Foss M, Villella A, Taylor BJ, Hall JC, Baker BS. 2005. Male-specific fruitless specifies the neural substrates of Drosophila courtship behaviour. *Nature*.

Nakayama S, Kaiser K, Aigaki T. 1997. Ectopic expression of sex-peptide in a variety of tissues in Drosophila females using the P[GAL4] enhancer-trap system. *Mol Gen Genet* **254**: 449-455.

Nallasivan MP, Haussmann IU, Civetta A, Soller M. 2021. Channel nuclear pore protein 54 directs sexual differentiation and neuronal wiring of female reproductive behaviors in Drosophila. *BMC biology* **19**: 226.

Nojima T, Rings A, Allen AM, Otto N, Verschut TA, Billeter JC, Neville MC, Goodwin SF. 2021. A sex-specific switch between visual and olfactory inputs underlies adaptive sex differences in behavior. *Curr Biol* **31**: 1175-1191.e1176.

Oliveira-Ferreira C, Gaspar M, Vasconcelos ML. 2023. Neuronal substrates of egg-laying behaviour at the abdominal ganglion of Drosophila melanogaster. *Sci Rep* **13**: 21941.

Peng J, Chen S, Busser S, Liu H, Honegger T, Kubli E. 2005. Gradual Release of Sperm Bound Sex-Peptide Controls Female Postmating Behavior in Drosophila. *Current Biology* **15**: 207-213.

Pfeiffer BD, Jenett A, Hammonds AS, Ngo TT, Misra S, Murphy C, Scully A, Carlson JW, Wan KH, Laverty TR et al. 2008. Tools for neuroanatomy and neurogenetics in Drosophila. *Proc Natl Acad Sci U S A* **105**: 9715-9720.

Phelps JS, Hildebrand DGC, Graham BJ, Kuan AT, Thomas LA, Nguyen TM, Buhmann J, Azevedo AW, Sustar A, Agrawal S et al. 2021. Reconstruction of motor control circuits in adult Drosophila using automated transmission electron microscopy. *Cell* **184**: 759-774.e718.

Rezaval C, Pavlou HJ, Dornan AJ, Chan YB, Kravitz EA, Goodwin SF. 2012. Neural circuitry underlying Drosophila female postmating behavioral responses. *Curr Biol* **22**: 1155-1165.

Riabinina O, Vernon SW, Dickson BJ, Baines RA. 2019. Split-QF System for Fine-Tuned Transgene Expression in Drosophila. *Genetics* **212**: 53-63.

Ribeiro C, Dickson BJ. 2010. Sex peptide receptor and neuronal TOR/S6K signaling modulate nutrient balancing in Drosophila. *Curr Biol* **20**: 1000-1005.

Rideout EJ, Dornan AJ, Neville MC, Eadie S, Goodwin SF. 2010. Control of sexual differentiation and behavior by the doublesex gene in Drosophila melanogaster. *Nat Neurosci* **13**: 458-466.

Rings A, Goodwin SF. 2019. To court or not to court - a multimodal sensory decision in Drosophila males. *Current opinion in insect science* **35**: 48-53.

Sakurai A, Koganezawa M, Yasunaga K, Emoto K, Yamamoto D. 2013. Select interneuron clusters determine female sexual receptivity in Drosophila. *Nature communications* **4**: 1825.

Scheffer LK Xu CS Januszewski M Lu Z Takemura SY Hayworth KJ Huang GB Shinomiya K Maitlin-Shepard J Berg S et al. 2020. A connectome and analysis of the adult Drosophila central brain. *Elife* **9**.

Scheunemann L, Lampin-Saint-Amaux A, Schor J, Preat T. 2019. A sperm peptide enhances long-term memory in female Drosophila. *Sci Adv* **5**: eaax3432.

Schmidt T, Choffat Y, Klauser S, Kubli E. 1993. The *Drosophila melanogaster* SP: A molecular analysis of structure-function relationships. *J Insect Physiol* **39**: 361-368.

Schretter CE, Aso Y, Robie AA, Dreher M, Dolan MJ, Chen N, Ito M, Yang T, Parekh R, Branson KM et al. 2020. Cell types and neuronal circuitry underlying female aggression in Drosophila. *Elife* **9**.

Schutt C, Nothiger R. 2000. Structure, function and evolution of sex-determining systems in Dipteran insects. *Development* **127**: 667-677.

Seidner G, Robinson JE, Wu M, Worden K, Masek P, Roberts SW, Keene AC, Joiner WJ. 2015. Identification of Neurons with a Privileged Role in Sleep Homeostasis in Drosophila melanogaster. *Curr Biol* **25**: 2928-2938.

Singh DND, Soller M. 2025. Venerose: a nuptial gift with implications. *J Neurogenet* **39**: 1-3.

Soller M, Bownes M, Kubli E. 1997. Mating and Sex Peptide Stimulate the Accumulation Of Yolk In Oocytes Of Drosophila Melanogaster. *European Journal of Biochemistry* **243**: 732-738.

-. 1999. Control of oocyte maturation in sexually mature Drosophila females. *Dev Biol* **208**: 337-351.

Soller M, Haussmann IU, Hollmann M, Choffat Y, White K, Kubli E, Schafer MA. 2006. Sex-peptide-regulated female sexual behavior requires a subset of ascending ventral nerve cord neurons. *Curr Biol* **16**: 1771-1782.

Sorkaç A, Mo□neanu RA, Crown AM, Savaş D, Okoro AM, Memiş E, Talay M, Barnea G. 2023. retro-Tango enables versatile retrograde circuit tracing in Drosophila. *Elife* **12**.

Stockinger P, Kvitsiani D, Rotkopf S, Tirian L, Dickson BJ. 2005. Neural circuitry that governs Drosophila male courtship behavior. *Cell* **121**: 795-807.

Struhl G, Basler K. 1993. Organizing activity of wingless protein in Drosophila. *Cell* **72**: 527-540.

Sweeney ST, Broadie K, Keane J, Niemann H, O'Kane CJ. 1995. Targeted expression of tetanus toxin light chain in Drosophila specifically eliminates synaptic transmission and causes behavioral defects. *Neuron* **14**: 341-351.

Talay M, Richman EB, Snell NJ, Hartmann GG, Fisher JD, Sorkaç A, Santoyo JF, Chou-Freed C, Nair N, Johnson M et al. 2017. Transsynaptic Mapping of Second-Order Taste Neurons in Flies by trans-Tango. *Neuron* **96**: 783-795.e784.

Wainwright SM, Hopkins BR, Mendes CC, Sekar A, Kroeger B, Hellberg J, Fan SJ, Pavey A, Marie PP, Leiblich A et al. 2021. Drosophila Sex Peptide controls the assembly of lipid microcarriers in seminal fluid. *Proc Natl Acad Sci U S A* **118**.

Wang F, Wang K, Forknall N, Parekh R, Dickson BJ. 2020a. Circuit and Behavioral Mechanisms of Sexual Rejection by Drosophila Females. *Curr Biol* **30**: 3749-3760.e3743.

Wang F, Wang K, Forknall N, Patrick C, Yang T, Parekh R, Bock D, Dickson BJ. 2020b. Neural circuitry linking mating and egg laying in Drosophila females. *Nature* **579**: 101-105.

Wang K, Wang F, Forknall N, Yang T, Patrick C, Parekh R, Dickson BJ. 2021. Neural circuit mechanisms of sexual receptivity in Drosophila females. *Nature* **589**: 577-581.

White MA, Bonfini A, Wolfner MF, Buchon N. 2021. Drosophila melanogaster sex peptide regulates mated female midgut morphology and physiology. *Proc Natl Acad Sci U S A* **118**.

Yamada D, Ishimoto H, Li X, Kohashi T, Ishikawa Y, Kamikouchi A. 2018. GABAergic Local Interneurons Shape Female Fruit Fly Response to Mating Songs. *J Neurosci* **38**: 4329-4347.

Yamamoto D, Koganezawa M. 2013. Genes and circuits of courtship behaviour in Drosophila males. *Nat Rev Neurosci* **14**: 681-692.

Yang CH, Rumpf S, Xiang Y, Gordon MD, Song W, Jan LY, Jan YN. 2009. Control of the postmating behavioral switch in Drosophila females by internal sensory neurons. *Neuron* **61**: 519-526.

Yapici N, Kim YJ, Ribeiro C, Dickson BJ. 2008. A receptor that mediates the post-mating switch in Drosophila reproductive behaviour. *Nature* **451**: 33-37.

Zaharieva E, Haussmann IU, Brauer U, Soller M. 2015. Concentration and localization of co-expressed ELAV/Hu proteins control specificity of mRNA processing. *Mol Cell Biol* **35**: 3104-3115.

Zhang SX, Glantz EH, Miner LE, Rogulja D, Crickmore MA. 2021. Hormonal control of motivational circuitry orchestrates the transition to sexuality in Drosophila. *Sci Adv* **7**: eabg6926.

Zhou C, Pan Y, Robinett CC, Meissner GW, Baker BS. 2014. Central brain neurons expressing doublesex regulate female receptivity in Drosophila. *Neuron* **83**: 149-163.

Figure legends

Figure 1: The main PMRs in females can be separated.

A, B) Schematic depiction of head and trunk expression in *Drosophila elav FRTstopFRT GAL4*; *otdflp* (A) and in *tshGAL4* (B) visualized by *UAS GFP* (green).

C, D) Receptivity (C) and oviposition (D) of wild type control virgin (red) and mated (orange) females, and virgin females expressing *UAS mSP* (green) pan-neuronally with *nsybGAL4* or in head and trunk patterns shown as means with standard error from three repeats for receptivity (21 females per repeat) by counting the number of females mating within a 1 h period or for oviposition by counting the eggs laid within 18 hours from 30 females. Statistically significant differences from ANOVA post-hoc comparison are indicated by different letters ($p<0.0001$).

E-H) Representative adult female genital tract showing *tshGAL4 UAS H2BYFP* (green) and *elavLexA LexAop NLStomato* (red) nuclear expression. The magnification (F-H) shows sensory genital tract neurons. Scale bar shown in E and H are 100 μm and 20 μm, respectively.

Figure 2: Distinct regulatory regions in *SPR*, *fru* and *dsx* genes induce PMRs from mSP expression.

A-C) Schematic representation of *SPR*, *fru*, and *dsx* chromosomal regions depicting coding and non-coding exons as black or white boxes, respectively, and splicing patterns in solid lines. Vertical lines below the gene model depict enhancer *GAL4* lines with names and those in red showed PMRs by expression of mSP.

D, E) Receptivity (D) and oviposition (E) of wild type control virgin (red) and mated (orange) females, and virgin females expressing *UAS mSP* (green) under the control of GAL4 pan-neuronally in *nsyb* or in *SPR8*, *SPR12*, *fru11*, *fru12*, and *dsx24* patterns shown as means with standard error from three repeats for receptivity (21 females per repeat) by counting the number of females mating within a 1 h period or for oviposition by counting the eggs laid within 18 hours from 30 females. Statistically significant differences from ANOVA post-hoc comparison are indicated by different letters ($p\leq0.0001$).

F-O) Representative adult female brains (F-J) and ventral nerve cords (VNC, K-O) expressing *UAS CD8GFP* under the control of *SPR8*, *SPR12*, *fru11*, *fru12* and *dsx24 GAL4*. Scale bars shown in J and O are 50 µm and 100 µm, respectively.

Figure 3: Expression of mSP in secondary ascending abdominal ganglion neurons induces PMRs.

A, B) Receptivity (A) and oviposition (B) of wild type control virgin (red) and mated (orange) females, and virgin females expressing *UAS mSP* (green) under the control of GAL4 pan-neuronally in *nsyb* or in *FD1*, *FD2*, *FD3*, *FD4*, *FD5*, and *FD6*, or with *SAG split-Gal4* patterns shown as means with standard error from three repeats for receptivity (21 females per repeat) by counting the number of females mating within a 1 h period or for oviposition by counting the eggs laid within 18 hours from 30 females. Statistically significant differences from ANOVA post-hoc comparison are indicated by different letters ($p<0.0001$).

Figure 4: Distinct circuits from intersection of *SPR*, *fru*, *dsx* and *FD6* patterns in the brain and VNC induce PMRs from mSP expression.

A) Schematic showing the intersectional gene expression approach: GAL4 activation (AD, orange) and DNA binding domains (DBD, blue) are expressed in different, but overlapping patterns. Leucine zipper dimerization reconstitutes a functional split-GAL4 in the intersection (pink) to express *UAS* reporters.

B, C) Receptivity (B) and oviposition (C) of wild type control virgin (red) and mated (orange) females, and virgin females expressing *UAS mSP* (green) under the control of *split-GAL4* intersecting *SPR8* ∩ *fru11/12*, *SPR8* ∩ *dsx*, *SPR8* ∩ *FD6*, *fru11/12* ∩ *dsx* and *fru11/12* ∩ *FD6* patterns shown as means with standard error from three repeats for receptivity (21 females per repeat) by counting the number of females mating within a 1 h period or for

839 oviposition by counting the eggs laid within 18 hours from 30 females. Statistically
840 significant differences from ANOVA post-hoc comparison are indicated by different letters
841 ($p<0.0001$).

842 **D-M)** Representative adult female brains and ventral nerve cords (VNC) expressing *UAS*
843 *CD8GFP* under the control of *SPR8 ∩ fru11/12*, *SPR8 ∩ dsx*, *SPR8 ∩ FD6*, *fru11/12 ∩ dsx*
844 and *fru11/12 ∩ FD6*. Scale bars shown in H and M are 50 µm and 100 µm, respectively.

845

846 **Figure 5: Distinct neuronal circuitries from intersection of *SPR*, *fru* and *dsx* sense SP**
847 **after mating to induce PMRs.**

848 **A, B)** Receptivity (A) and oviposition (B) of wild type control virgin (red) and mated
849 (orange) females, and virgin females expressing *UAS mSP* (green) under the control of *split-*
850 *Gal4* intersecting *SPR8 ∩ dsx*, *fru11/12 ∩ dsx*, and *SPR8 ∩ fru11/12* patterns in *SPR/Df*
851 mutant females or *SPR* RNAi knock-down shown as means with standard error from three
852 repeats for receptivity (21 females per repeat) by counting the number of females mating
853 within a 1 h period or for oviposition by counting the eggs laid within 18 hours from 30
854 females. Statistically significant differences from ANOVA post-hoc comparison are indicated
855 by different letters ($p<0.0001$ except $p=0.002$ and $p=0.006$ for c and d in A, and $p=0.004$ for
856 c in B).

857

858 **Figure 6: Distinct neuronal circuitries in the brain sense SP to induce PMRs.**

859 **A, B)** Schematic depiction of *UAS GFP* (green) expression in the head of *Drosophila* (A)
860 combining *split-GAL4* intersectional expression (*AD-GAL4* and *GAL4-DBD*) with brain-
861 expressed *otdflp* mediated recombination of *UAS FRTGFPstopFRTmSP* (B).

862 **C, D)** Receptivity (C) and oviposition (D) of wild type control virgin (red) and mated
863 (orange) females, and virgin females expressing *UAS FRTGFPstopFRTmSP* (grey), *UAS*

FRTGFPstopFRTTrpA1 (purple) and *UAS FRTGFPstopFRTTNT* (pink) under the control of *split-GAL4* intersecting *SPR8* ∩ *dsx*, *fru11/12* ∩ *dsx* and *SPR8* ∩ *fru11/12* patterns with brain-specific FRT-mediated recombination by *otdflp* shown as means with standard error from three repeats for receptivity (21 females per repeat) by counting the number of females mating within a 1 h period or for oviposition by counting the eggs laid within 18 hours from 30 females. Statistically significant differences from ANOVA post-hoc comparison are indicated by different letters ($p<0.0001$ except $p<0.0004$ for c in C, $p<0.007$ for c in D).

Figure 7: *retro*- and *trans*-Tango identification of pre- and post-synaptic neurons of SP target neurons reveals higher order neuronal input canalized into shared output circuitries.

A-O) Representative adult female brains expressing *QUAST tomato3xHA retro*-Tango (left, A-E), *UAS myrGFP* (middle, F-J) and *QUAST tomato3xHA trans*-Tango (right, K-O) in *SPR8* ∩ *dsx*, *fru11/12* ∩ *dsx* , *SPR8* ∩ *fru11/12*, *SPR8* ∩ *FD6* and *fru11/12* ∩ *FD6* split-*GAL4s*. The presynaptic (A-E, left), *split-GAL4* (F-J, middle) and postsynaptic (K-O, right) neuronal circuitries are shown in an inverted grey background. Arrows (magenta) indicate neurons and their corresponding projections in different regions in female brain. The scale bar shown in O is 50 μm.

P) Model for the SP induced post-mating response. SP interferes with interpretation of sensory cues, e.g. vison, hearing, smell, taste, and touch at distinct sites in the brain indicated by higher order projections revealed by intersectional expression in the following patterns: *SPR8* ∩ *dsx* (blue), *fru11/12* ∩ *dsx* (black), *SPR8* ∩ *fru11/12* (yellow), *SPR8* ∩ *FD6* (pink) and *fru11/12* ∩ *FD6* (olive). and VNC (*fru11/12* ∩ *dsx*) during higher order neuronal processing.

889 **Supplementary information**

890 **Supplementary Figure S1: Analysis of head and trunk expression lines.**

891 **A-F)** Expression of *UAS CD8 GFP* driven *elav FRTstopFRT GAL4* restricted with *otdflp* to
892 the head in the brain and VNC.

893 **G-L)** Expression of *tshGAL4 UAS H2B YFP* with neurons labeled with tomato from
894 *elavLexA AopNLStomato* in the brain and VNC.

895

896 **Supplementary Figure S2: Expression analysis of PMR-inducing *GAL4* in the genital**
897 **tract.**

898 **A-E)** Representative adult female genital tracts expressing *UAS CD8GFP* under the control
899 of *SPR8*, *SPR12*, *fru11*, *fru12* and *dsx24 GAL4*, and *LexAop NLStomato* under the control of
900 *elavLexA*. Arrows indicate genital tract sensory neurons. The insert shows expression of GFP
901 in the genital tract sensory neurons. Scale bars shown in A and insets are 100 µm and 20 µm,
902 respectively.

903

904 **Supplementary Figure S3: Expression analysis of non-PMR-inducing *fru9GAL4* in the**
905 **genital tract.**

906 Representative adult female genital tract expressing *UAS CD8GFP* under the control of *fru9*
907 *GAL4*. Arrows indicate genital tract sensory neurons. The insert shows expression of GFP in
908 the genital tract sensory neurons. Scale bars shown in C and insets are 100 µm and 20 µm,
909 respectively.

910

911 **Supplementary Figure 4: Expression of mSP in *SPSN*, and genital tract expression *SPR***
912 **lines does not support a major role for genital tract neurons in inducing the sex peptide**
913 **response.**

A, B) Receptivity (A) and oviposition (B) of wild type control virgin (red) and mated (orange) females, and virgin females expressing *UAS mSP* (green) under the control of *SPSN 1* and *SPSN2*, and *and SPR3* and *SPR9 GAL4* lines shown as means with standard error from three repeats for receptivity (21 females per repeat) by counting the number of females mating within a 1 h period or for oviposition by counting the eggs laid within 18 hours from 30 females. Statistically significant differences from ANOVA post-hoc comparison are indicated by different letters ($p<0.0001$).

C-J) Representative genital tracts labelled with UAS CD8 GFP and genital tract neurons labelled with UAS H2BYFP and *elavLexA AopNLStomato*.

K-R) Adult female brains (K-N) and ventral nerve cords (VNC. O-R) expressing *UAS CD8GFP*. Scale bars shown in H and M are 50 µm and 100 µm, respectively.

Supplementary Figure S5: Expression analysis of split-GAL4 in the genital tract.

A-E) Representative adult female genital tracts expressing *UAS CD8GFP* under the control of *SPR8 ∩ fru11/12, SPR8 ∩ dsx, SPR8 ∩ FD6, fru11/12 ∩ dsx* and *fru11/12 ∩ FD6 split-GAL4* intersectional patterns. The scale bar shown in E is 100 µm.

Supplementary Figure S6: Expression analysis of split-GAL4 in the genital tract.

A-C) Visualisation of single cell expression for *CG31637* intersected with *SPR, fru* and *dsx*.

D-F) Visualisation of single cell expression for *ocelliless* intersected with *SPR, fru* and *dsx*.

G-I) Visualisation of single cell expression for *Gyc76c* intersected with *SPR, fru* and *dsx*.

Supplementary Figure 7: Expression of mSP in *SPSN VT058873 AD* intersected with *SPR8 DBD, fru11/12 DBD* and *dsx DBD* induces PMRs and *SPSN VT058873 AD* intersected with *SPR8 DBD* and *dsx DBD* sense SP in the brain.

939 **A, B)** Receptivity (A) and oviposition (B) of wild type control virgin (red) and mated
940 (orange) females, and virgin females expressing *UAS mSP* (green) under the control of
941 *VT058873 ∩ SPR8, VT058873 ∩ fru11/12 and VT058873 ∩ dsx* shown as means with
942 standard error from three repeats for receptivity (21 females per repeat) by counting the
943 number of females mating within a 1 h period or for oviposition by counting the eggs laid
944 within 18 hours from 30 females. Statistically significant differences from ANOVA post-hoc
945 comparison are indicated by different letters ($p<0.0001$).
946 **C-H)** Adult female brains (C-E) and ventral nerve cords (VNC, F-H) expressing *UAS*
947 *CD8GFP*. Scale bars shown in H and M are 50 µm and 100 µm, respectively.
948 **I-N)** Representative genital tracts labelled with UAS CD8 GFP and genital tract neurons
949 labelled with *UAS H2BYFP* and *elavLexA AopNLStomato*.
950 **O, P)** Receptivity (O) and oviposition (P) of wild type control virgin (red) and mated
951 (orange) females, and virgin females expressing *UAS FRTGFPstopFRTmSP* (grey) and *UAS*
952 *FRTGFPstopFRTTrpA1* (purple) under the control of *split-GAL4* intersecting *VT058873 ∩*
953 *SPR8, VT058873 ∩ fru11/12 and VT058873 ∩ dsx* patterns with brain-specific FRT-mediated
954 recombination by *otdflp* shown as means with standard error from three repeats for
955 receptivity (21 females per repeat) by counting the number of females mating within a 1 h
956 period or for oviposition by counting the eggs laid within 18 hours from 30 females.
957 Statistically significant differences from ANOVA post-hoc comparison are indicated by
958 different letters ($p<0.0001$).
959
960 **Supplementary Figure S8: *ppk* is not part of the *SPR8, SPR12 and fru11/12* PMR-**
961 **inducing neuronal circuitry**
962 **A, B)** Receptivity (A) and oviposition (B) of wild type control virgin (red) and mated
963 (orange) females, and virgin females expressing *UAS mSP* (green) under the control of *GAL4*

964 in *ppk* or in *nSyb* ∩ *ppk, SPR8* ∩ *ppk, SPR12* ∩ *ppk,* and *fru11/12* ∩ *ppk* patterns shown as
965 means with standard error from three repeats for receptivity (21 females per repeat) by
966 counting the number of females mating within a 1 h period or for oviposition by counting the
967 eggs laid within 18 hours from 30 females. Statistically significant differences from
968 ANOVA post-hoc comparison are indicated by different letters ($p<0.0001$).
969 **C-R)** Representative adult female brains, ventral nerve cords (VNC) and genital tracts
970 expressing *UAS CD8GFP* under the control of *UAS* by *nSyb* ∩ *ppk, SPR8* ∩ *ppk, SPR12* ∩
971 *ppk,* and *fru11/12* ∩ *ppk*. Scale bars shown in E are 50 µm and in H and K are 100 µm,
972 respectively.
973 **S-V)** Receptivity (S, T) and oviposition (U, V) of wild type control virgin (red) and mated
974 (orange) females, and virgin females expressing either *UAS TNT* (azure) or *UAS NaChBac*
975 (brown) to inhibit or activate neurons in *SPR8* ∩ *ppk, SPR12* ∩ *ppk,* and *fru11/12* ∩ *ppk*
976 patterns shown as means with standard error from three repeats for receptivity (21 females
977 per repeat) by counting the number of females mating within a 1 h period or for oviposition
978 by counting the eggs laid within 18 hours from 30 females. Statistically significant
979 differences from ANOVA post-hoc comparison are indicated by different letters ($p<0.001$ for
980 b, and $p<0.01$ for c in L and N).
981
982 **Supplementary Figure 9: Expression of mSP in female reproductive behavior**
983 **regulating neuron *split-GAL4* lines.**
984 **A, B)** Receptivity (A) and oviposition (B) of wild type control virgin (red) and mated
985 (orange) females, and virgin females expressing *UAS mSP* (green) under the control of *pC1-*
986 *SS1, oviDN-SS1 and 2, oviEN-SS1 and 2, oviIN-SS1 and 2, and vpoDN-SS1* shown as means
987 with standard error from three repeats for receptivity (21 females per repeat) by counting the
988 number of females mating within a 1 h period or for oviposition by counting the eggs laid

within 18 hours from 30 females. Statistically significant differences from ANOVA post-hoc comparison are indicated by different letters ($p<0.0001$).

C-J) Representative genital tract neurons labelled with *UAS H2BYFP* and *elavLexA AopNLStomato*.

Supplementary Figure S10: PMRs after neuronal inhibition, ablation or activation of distinct circuits from intersection of *SPR*, *fru*, *dsx* and *FD6* patterns in the brain and VNC.

A-F) Receptivity (A, C and E) and oviposition (B, D and F) of wild type control virgin (red) and mated (orange) females, and virgin females expressing either *UAS TNT* (azure, A and B) or *UAS reaper hid* to inhibit or ablate neurons (yellow, C and D), respectively, or *UAS NaChBac* (brown, E and F) to activate neurons in *SPR8* ∩ *fru11/12*, *SPR8* ∩ *dsx*, *SPR8* ∩ *FD6*, *fru11/12* ∩ *dsx* and *fru11/12* ∩ *FD6 split-Gal4* patterns shown as means with standard error from three repeats for receptivity (21 females per repeat) by counting the number of females mating within a 1 h period or for oviposition by counting the eggs laid within 18 hours from 30 females. Statistically significant differences from ANOVA post-hoc comparison are indicated by letters ($p\leq0.0095$ in A and B, $p<0.0001$ in C and D except $p=0.016$ for c in D, $p<0.0001$ in E and $p<0.0002$ in F).

Supplementary Figure S11: *trans*-Tango identifies post-synaptic proceeding neurons of SP targets in the VNC, but not the genital tract

A-AD) Representative adult female ventral nerve cords (VNC, A-O) and genital tracts (P-AD) expressing *UAS myrGFP; QUAST tomato3xHA trans*-Tango in *SPR8* ∩ *fru11/12*, *SPR8* ∩ *dsx*, *SPR8* ∩ *FD6*, *fru11/12* ∩ *dsx* and *fru11/12* ∩ *FD6* split-*GAL4s*. The presynaptic (A-E and P-T) and postsynaptic (F-J and U-Y) neuronal circuitries are shown in an inverted grey

1014 background and the merge is shown in colour. In the merged picture (K-O and Z-AD), the
1015 pre-synaptic and post synaptic neuronal circuitry is shown in green and magenta,
1016 respectively. Scale bars shown in O and AD are 100 μm.
1017

Figure 1

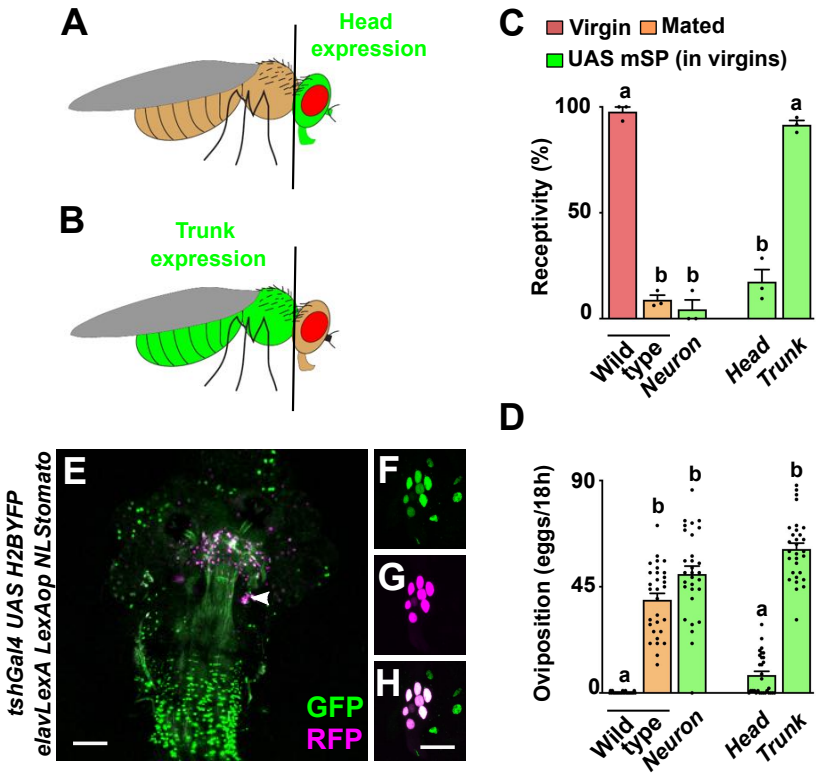

Figure 2

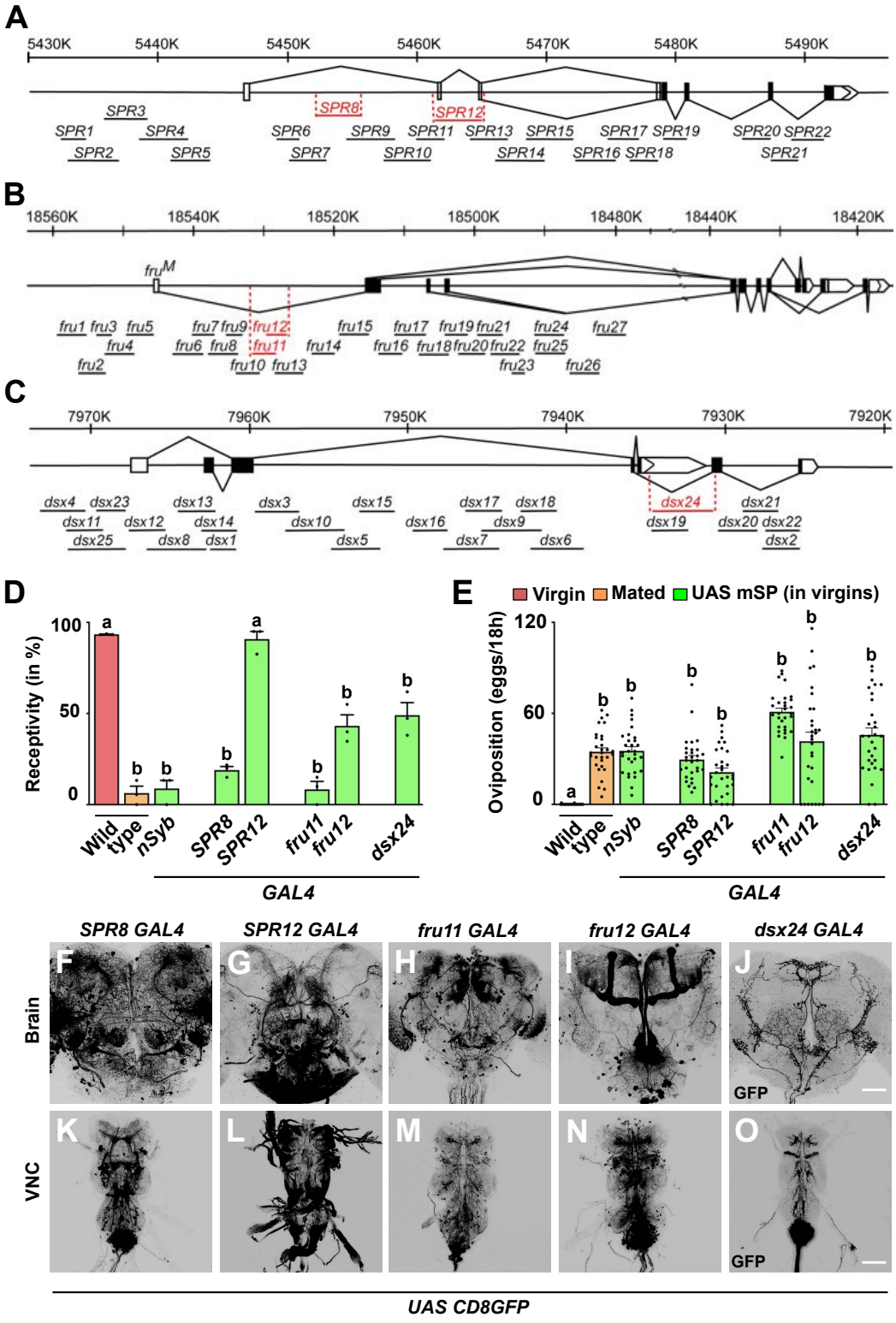

Figure 3

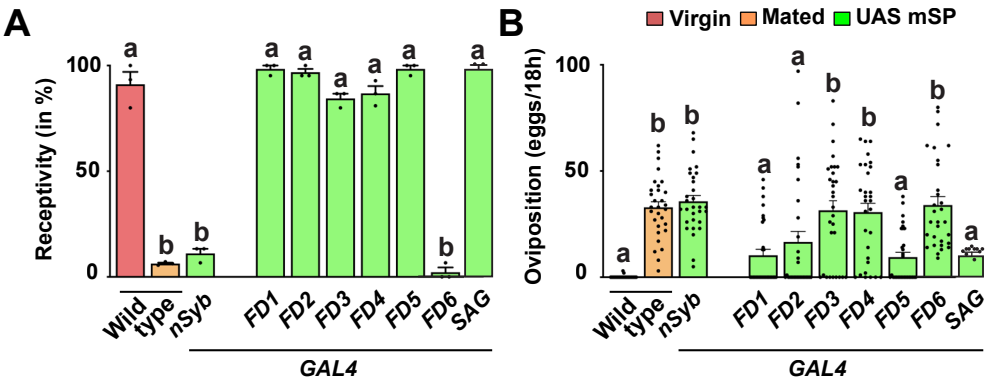

Figure 4

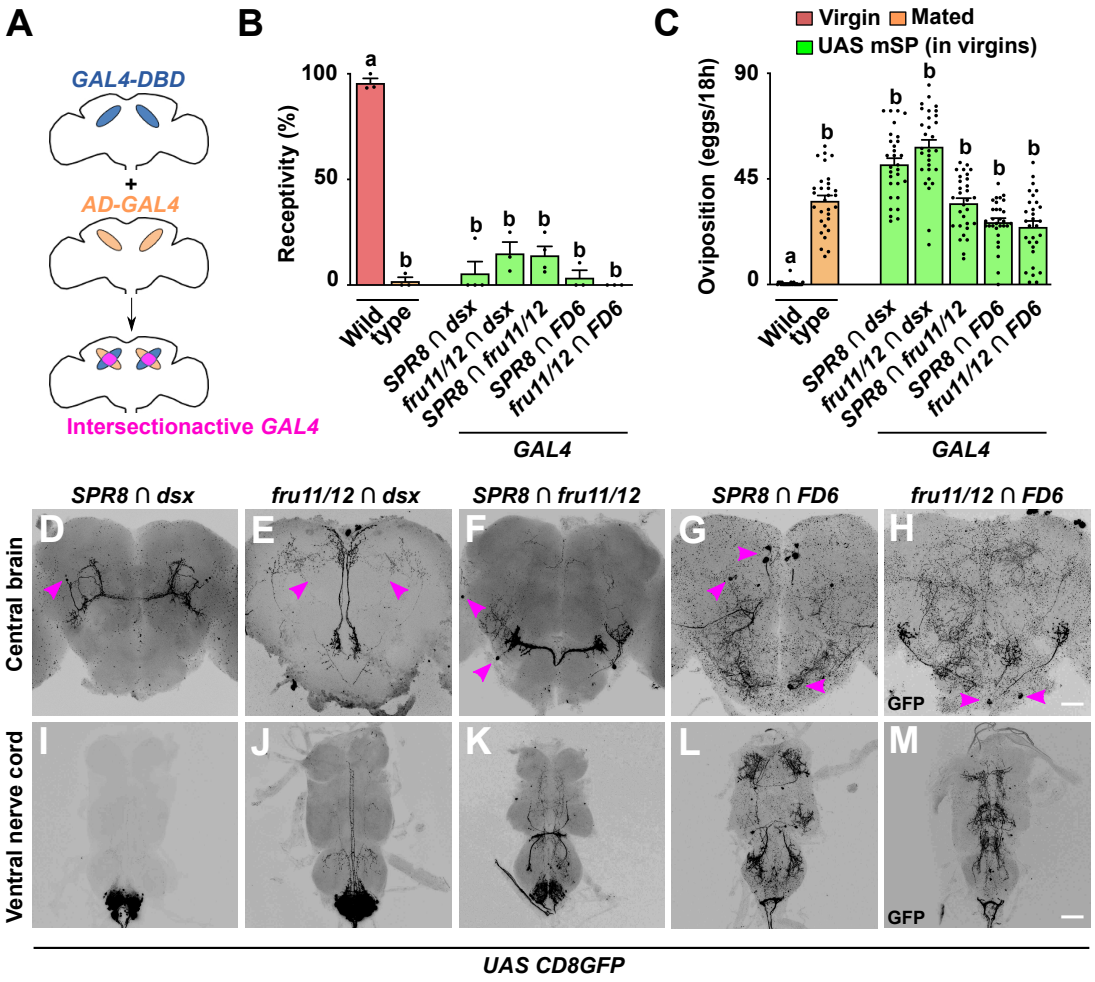

Figure 5

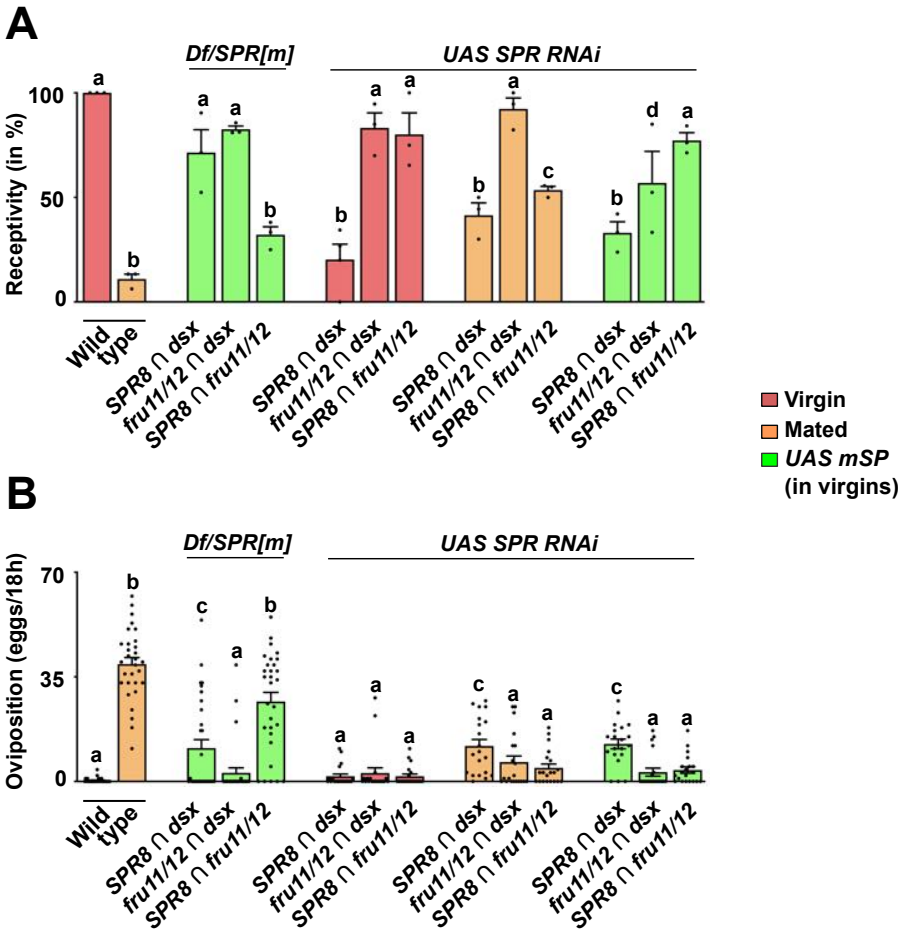

Figure 6

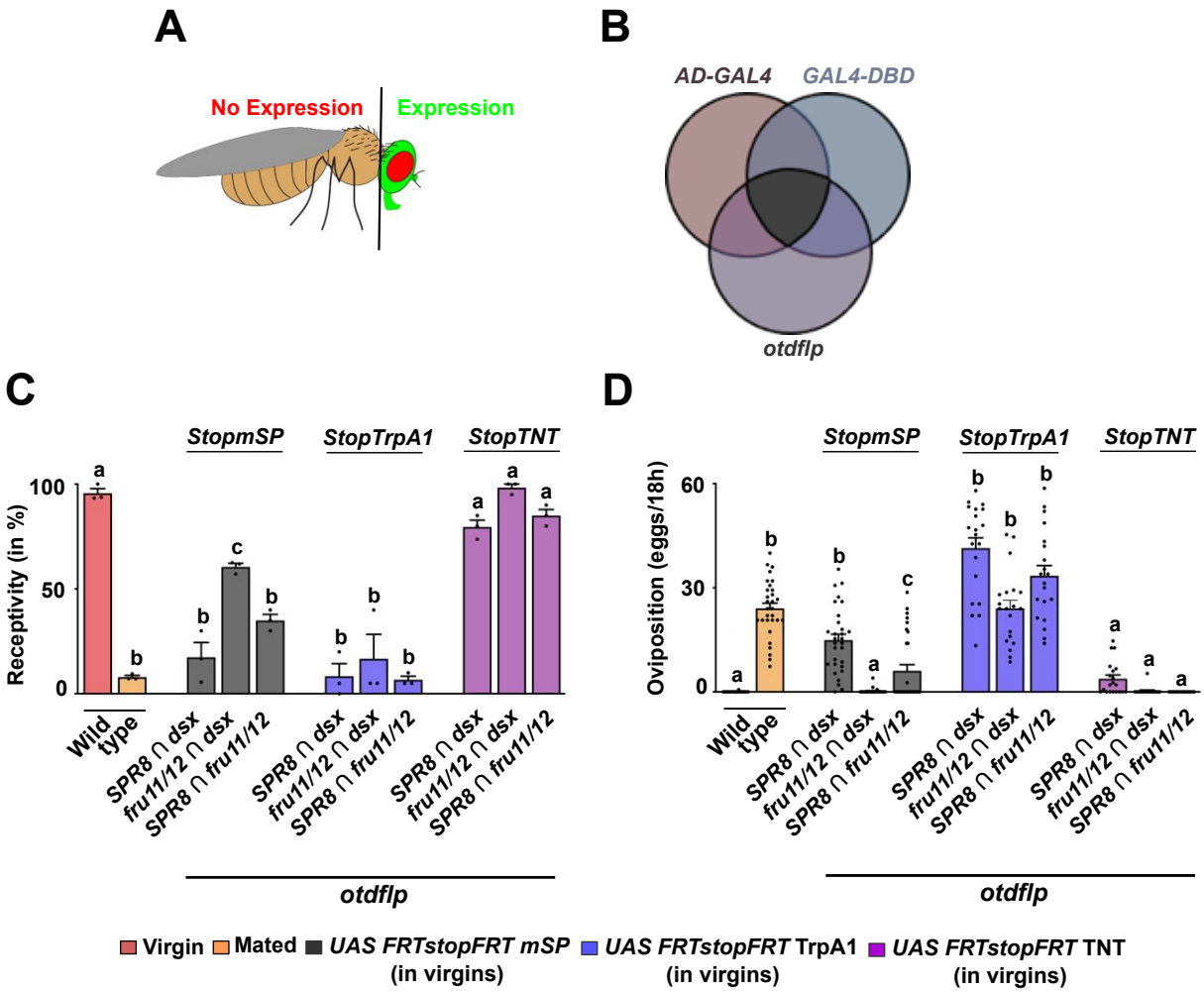

Figure 7

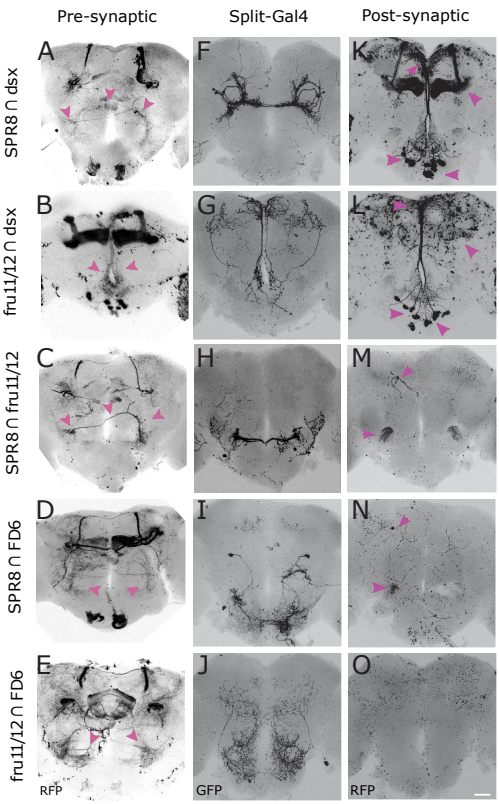
Pre-synaptic
Split-Gal4
Post-synaptic
SPR8 ∩ dsx
fru11/12 ∩ dsx
SPR8 ∩ fru11/12
SPR8 ∩ FD6
fru11/12 ∩ FD6
A
B
C
D
E
F
G
H
I
J
K
L
M
N
O
RFP
GFP
RFP

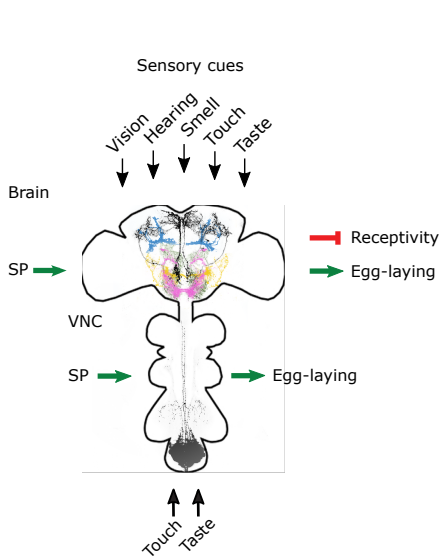
P
Sensory cues
Vision
Hearing
Smell
Touch
Taste
Brain
SP
Receptivity
Egg-laying
VNC
SP
Egg-laying
Touch
Taste